

White paper

VIVID - German Japan Joint Virtual Validation Methodology for Intelligent Driving Systems



December 27, 2023

Authors: Philip Aust, Yoshihisa Amano, Atsushi Araki, Lukas Elster, Lukas Haas, Arsalan Haider, Matthias A. Hein, Norihito Hiruma, Hasan Iqbal, Takashi Kaneshiro, Aidar Khakimov, Michael Köhler, Viktor Lizenberg, Masashi Mizukoshi, Wataru Nakamura, Masami Nerio, David Nickel, Mario Pauli, Michael Schardt, Stefan-Alexander Schneider, Toshinobu Sugiyama, Thomas Zeh

Editors: Kazuhiko Hanaya, Ken Mori, Riki Sawamura, Matthias A. Hein, and Hideo Inoue

Content

1. Introduction.....	1
1.1. Motivation and outline.....	1
1.2. Objectives and Approaches.....	1
2. Project overview	2
2.1. Overview across all JT.....	2
2.2. X-Model.....	4
2.3. Safety assurance framework.....	6
3. Modeling outline	7
3.1. A structure and study process for physical sensor modeling	7
3.2. Segmentation with decomposition applied in DIVP® and VIVALDI.....	9
3.3. Extracting requirements from sensor perception effects	10
4. Modeling process and results.....	12
4.1. Environment modeling	12
4.2. Propagation modeling.....	14
4.3. Sensor modeling.....	16
4.4. Model/data exchange and interfaces for standardization	21
5. Validation process	23
5.1. Validation of model constituents (Laboratory).....	24
5.2. Validation of integrated model (installed performance on a real vehicle).....	26
5.3. Validation of consistency and safety argumentation.....	29
6. Summary of key results and conclusions.....	32
6.1. Summary of key results.....	32
6.2. Conclusion.....	32

1. Introduction

This document outlines the shared approach and joint achievements of the German-Japanese research cooperation VIVID – “German Japan joint virtual validation methodology for intelligent driving systems”, which combines the two sister projects VIVALDI (German partners) “Virtual validation toolchain for automated and connected driving” and DIVP® (Japanese partners): “Driving intelligence validation platform”, funded by the German BMBF (coordinated by TU Ilmenau, 16 ME 0164 K) and the CAO (Japanese Cabinet Office) and METI (Ministry of Economy, Trade and Industry) under the bi-national research cooperation on connected and automated driving. This section introduces motivation, objectives, and an overview of the research cooperation.

1.1. Motivation and outline

Connected and automated driving (CAD) requires the highest level of safety for the vehicles and their driving functions. Technological pre-requisites concern a comprehensive environmental perception based on complementary as well as redundant sensor systems and reliable wireless communication with control centers or other vehicles, road infrastructure, and traffic participants.

Safety assurance is of major concern for the development and eventual homologation of connected and automated cars. Previous projects, especially the PEGASUS project family, proposed scenario-based testing as a valid alternative paradigm to distance-based safety validation.¹ This approach is particularly suited in combination with virtual testing in simulation. Virtual methods enable scalable, efficient, and reproducible test capabilities compared to field-operational testing for the safety assurance of CAD.

Virtual verification and validation is becoming one important method in upcoming safety standards². The German-Japanese research cooperation VIVID^{3,4} focuses on scenario-based safety assurance along a complete simulation tool chain. It also aims at strengthening the exchange of knowhow through joint research and development at a pre-competitive level with the goal to reach global harmonization and move towards international standardization.

1.2. Objectives and Approaches

VIVID addresses the key question: "How can the safety of CAD driving functions be tested, measured, and assured?" Virtual test environments reaching from software-in-the-loop (SiL) through over-the-air vehicle-in-the-loop (OTA/ViL) up to test drives on proving grounds and field-operational tests (FoT) on public roads have been developed for camera, lidar, and radar sensors. The methods include sensor reference data as well as sensor and environmental models, embedded into holistic simulation tool chains. The project investigates how close to reality such simulations

¹ <https://www.pegasusprojekt.de/en/pegasus-method>

² European Commission: Automated cars – technical specifications, draft, available online: https://ec.europa.eu/info/law/better-regulation/have-your-say/initiatives/12152-Automated-cars-technical-specifications_en

³ <https://divp.net/>

⁴ <https://www.safecad-vivid.net/>

JT	Elements		
1	Tool chain		
2	Scenario/ Camera	 	 
3	LiDAR		
	Radar		
4	Measurement&Metrics		

Figure 1-1: Overview of the VIVID joint topical task teams and their lead institutions'

in a virtual environment can reach, and to what extent they can represent the complexity of field-operational tests. The cooperation delivers on one hand added value through commonalities such as convergence between models and interfaces. On the other hand, complementarities regarding model portfolios as well as different expertise and approaches are exploited. The binding link between both consortia was provided by six joint topical task teams (JT) as depicted in Figure 1-1.

2. Project overview

This section provides an overview of the VIVID project. The collaboration within the different JT is described at first, followed by a presentation of the X-Model which provides the structural background in which the project is embedded. Finally, the safety assurance framework of VIVID is described.

2.1. Overview across all JT

The Japanese DIVP⁵ and the German VIVALDI⁶ sister projects have jointly worked towards a harmonized virtual validation framework and global standardization with a focus on open interfaces and data formats for mutual exchange. Based on the DIVP⁵ safety assurance strategy, each process along the simulation toolchain, including a scenario generator and raytracing-based propagation modeling, and a sensor validation platform, is based on expert knowledge. So far, camera perception interfaces were already standardized. For scenarios and environmental models including material properties, a joint format has been identified, while the model interfaces for radar sensors have been accepted for the OpenX standard family by ASAM⁷.

Major achievements have become possible through intense cooperation in the framework of the six joint topical task teams. Figure 2-1 depicts the interplay of the different JT within the joint validation framework established through VIVID.

⁵ <https://divp.net/>

⁶ <https://www.safecad-vivid.net/>

⁷ <https://www.asam.net/standards/>

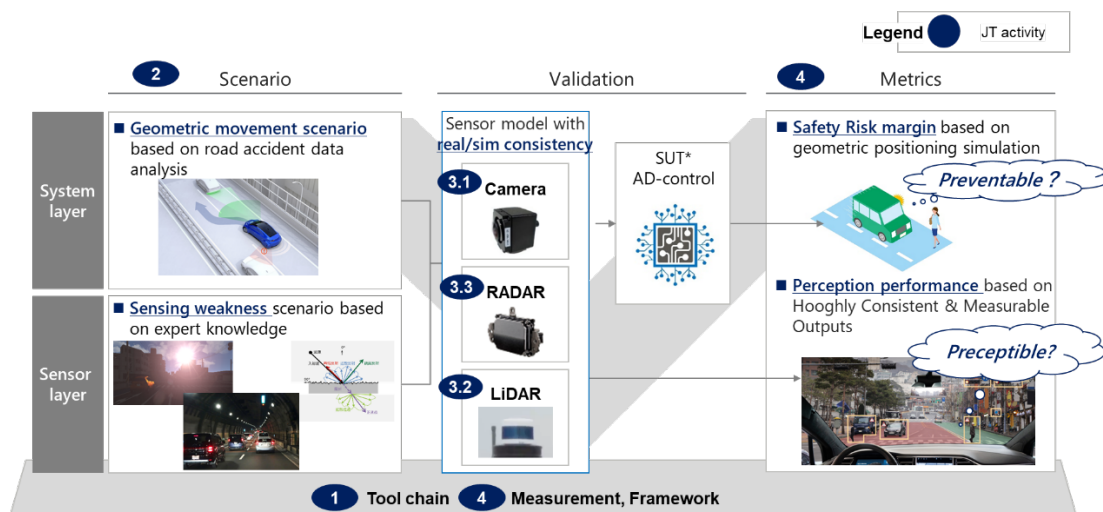


Figure 2-1: Total validation framework for AD-safety assurance with the international cooperation indicated by the six JT according to Fig. 1-1.

Each JT consisted of expert members of both project consortia who collaborated and exchanged technical solutions with each other via frequent dedicated meetings. The interchangeable implementation and re-processing of environmental and sensor data allowed for a reconstruction, and analysis, as well as future mitigation, of adverse effects in a controlled and safe environment. In JT2, selected sensing weakness scenarios provoked, e.g., by lighting (esp. stray light and backscattering) or weather conditions (esp. precipitation like rain and fog) were exchanged successfully, thanks to common data formats and adapted simulation interfaces. A common material database addressing the three grossly different wavelength ranges inherent to the sensor modalities (camera: visible light, lidar: near infrared, radar: millimeter waves) has been established and is openly available for further use and extension, in combination with a proposal to integrate the highly relevant electrodynamic materials properties through OpenMaterial into the OpenX standard family. The three sensor-related JT3 teams (3.1 camera, 3.2 lidar, and 3.3 radar) succeeded in exchanging mutual data between the DIVP® environmental model and the VIVALDI sensor models, ready for interface standardization. Especially for camera, the connectivity between DIVP® data, based on a physical model architecture converted to OSI format, and the VIVALDI platform, based on a behavioral model architecture, could be verified. For radar sensor modeling, ray tracing data of scenario-specific propagation models could be successfully exchanged between DIVP® and VIVALDI. Within JT4, a mutual understanding of the processes and methodologies involved has been reached, aiming at de-facto standardization. The next steps aim at defining and disseminating a consistent AD safety assurance standard, the “VIVID standard”. Further activities of JT4 address the highly relevant issue of metrics for the validation of the underlying models and the entire simulation toolchain. Connecting to other major global R&D activities on safety assurance of CAD will eventually provide maximum benefit.

Despite the Corona pandemic, the lively VIVID cooperation included two international in-person conferences in 2022, namely the safeCAD-DJ symposium held in June in Berlin, and the SIP-adus workshop in October in Kyoto, each attended by about 20 participants from the invited partner projects. The vivid discussions of major regional activities in the United States of America, the European Union, and in Japan at the SIP-adus workshop revealed the advanced status reached by the VIVID consortium, setting the scene for global safety assurance activities including the PEGASUS project family⁸ and, more recently, the “Closing the gap” initiative of the SafeTrans association⁹, working on a roadmap “Controlling risk for highly automated transportation systems operating in complex open environments – CONTROL”. Future research would need to address cross-domain, technology-agnostic, and adaptable sensor and environmental models. This includes 5G/6G connectivity and sensor data fusion, high-definition digital twins including all relevant interaction properties, seamless exchangeability between toolchains and between virtual and real worlds, and quality metrics for data-driven modeling. All of these topics will allow the global society to benefit from safe, clean, and efficient mobility in daily experience.

2.2. X-Model

This section aims at providing the conceptual VIVID framework. Within and across the two partner consortia, the field of research is structured in the form of a generic multi-layer, multi-domain model which is described in the following.

The shift-of-paradigm from distance-based towards scenario-based safety assurance⁸ in combination with the shift from real-world testing to virtual test environments inevitably compromises the closeness to reality and hence poses key questions like: „How X is X enough?”, where the placeholder X could read as “realistic”, “evident”, “consistent”, “justifiable”, “credible”, or “safe”. In consequence, the formulation of safety guarantees for CAD functions rests on a systematic and plausible safety argumentation. At the same time, the wealth of R&D activities worldwide, including large-scale industrial-academic consortia like VVM¹⁰, SetLevel¹¹, and VIVID¹², needs to be considered in a holistic context. An abstraction scheme adapted from the proven Y-model developed in the 1980-ties for VLSI hardware design¹³ presents a powerful descriptive approach to meet these requirements.

As displayed in Figure 2-2, the backbone of the X-model is formed by four constituting axes, arranged like the letter “X”. The four complementary pillars represent the variable, feasible, and efficient process steps towards safety assurance as such (upper left axis, dark blue), the definition and composition of scenarios (record, replay, re-arrange) forming the basis for safety testing (upper right, turquoise), the environmental perception resulting from the sensors under consideration and their models including sensor-specific limitations and weaknesses as well as metrics for model

⁸ <https://www.pegasusprojekt.de/en/pegasus-method>

⁹ <https://www.safetrans-de.org/en/index.php>

¹⁰ <https://www.vvm-projekt.de/en/>

¹¹ <https://setlevel.de/en>

¹² <https://www.safecad-vivid.net/>

¹³ D. D. Gajski and R. H. Kuhn. Guest Editor’s Introduction: New VLSI Tools. IEEE Computer, 1983

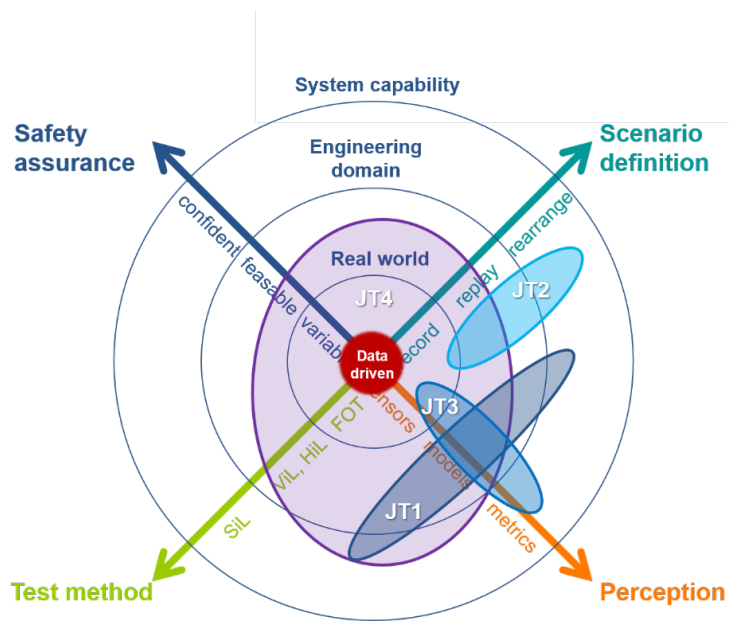


Figure 2-2: Graphical illustration of the X-model. The four axes denote the complementary pillars: Safety assurance (dark blue), scenario definition (blue-green), perception (orange), and test method (light green). The concentric circles denote abstraction layers, starting from the real world (inner circle), surrounded by the engineering domain (central layer) and a generic description of the system capability (outer layer). The red dot in the center represents expert knowledge. The numbered ellipses indicate the contributions from the joint topical task teams: JT1 (dark blue), JT2 (light blue), JT3 (blue), JT4 (purple). Further explanations are provided in the main text.

validation (lower right, orange), and the test modalities spanning all the way from field-operational testing (FoT) over hardware-in-the-loop (HiL) and vehicle-in-the-loop (ViL) up to the most generic software-in-the-loop (SiL) methods (lower left, light green). All four axes originate from the real world (red dot in Figure 2-2), accessible through reference measurements and expert knowledge only, and are connected with each other through successive abstraction layers (concentric circles in Figure 2-2). (For comparison, in the original Y-model, the three axes represent the electronic circuit domains behavior, structure, and geometry for the hardware design of integrated circuits.) Each of the four pillars proceeds through the engineering domain that enables modeling, simulating, or emulating the real-world behavior with a degree of fidelity that can be considered sufficiently high to formulate safety guarantees. The outermost circle provides the resulting world model and describes the performance on the system level. (For comparison, in the original Y-model, the abstraction layers develop from the circuit layer (innermost domain) over the logical and algorithmic layers towards the system layer.)

To meet the objective of a safety argumentation requires covering the entire domain space. Obviously, open and harmonized interfaces, open-access data repositories, and dedicated global standards form essential pre-requisites for a seamless combination of, and interaction between, different R&D activities, industrial test processes, and worldwide homologation efforts contributing to a continuous coverage of the domain space.

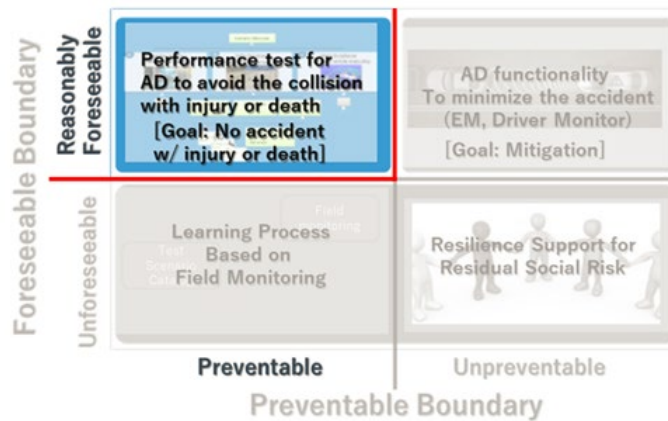


Figure 2-3: Safety principles for automated driving

The cooperation and topical interaction between the German and Japanese industrial-academic consortia in the VIVID-framework benefitted from the joint task teams introduced in section 2.1. Their topical areas can be mapped onto the X-diagram as indicated in Figure 2-2. The ensemble of activities and achievements covers a significant part of the domain space, with a dedicated focus on the two inner abstraction layers, forming the basis for physical sensor modeling, testing, and validation. At the same time, the achievements of VIVID represent a relevant complement of previous research activities (see footnotes^{6,7,8} and references therein) and deliver significant added value through the international cooperation and joint contributions to an open-standard ontology¹⁴ that is compatible with the structured approach inherent to the X-model.

2.3. Safety assurance framework

The VIVID safety assurance framework is illustrated in Figure 2-3 and further detailed below. One of the main features of the scenarios is not only the capability of reading traffic flow scenarios in the ASAM¹⁵ standard OpenDRIVE and OpenSCENARIO¹⁶ formats, but also the creation of sensing weakness scenarios to define sensor-specific perception. The sensing weakness scenario is a database of events derived from the knowledge and experience of experts, and high-priority scenarios have been determined and modeled based on a failure mode and effects (FMEA) analysis for each sensor.

The safety metrics for CAD are based on the definitions established by the United Nations' World forum for the harmonization of vehicle regulations UN/WP29¹⁷ and are divided into two-stage metrics: Recognition level and conflict risk level for traffic participants: "Automated vehicles shall not cause any non-tolerable risk, meaning that, under their operational domain, shall not cause any traffic accidents resulting in injury or death that are reasonably foreseeable and preventable."

¹⁴ <https://www.asam.net/project-detail/asam-openxontology/>

¹⁵ <https://www.asam.net/>

¹⁶ <https://www.asam.net/standards/detail/openscenario/>

¹⁷ UN/WP29, 2019, WP29-177-19, Framework document on automated/autonomous vehicles

These two key constituting elements, scenarios and metrics, are embodied in the safety assurance framework, which is more effective in reproducing the physical model of sensor perception in virtual space, a feature that has been developed in VIVID. From the recognition metrics, it is possible to determine critical priority scenarios that include parameters narrowed down from the evaluation of recognition limits. In addition, the timing of object recognition can be derived realistically from traffic environment scenarios, and the final safety risk level for object recognition can be quantitatively evaluated from their positions and relative speeds using time-to-collision (TTC) and post-encroachment time (PET) indicators.

Thus, the safety assurance framework structure based on a physical sensor perception model can contribute to safety assessment in terms of efficiency and reproducibility for connected and automated vehicles.

3. Modeling outline

Firstly, the overall process for sensor modeling is described. This is followed by a description of the decomposition approach applied to the environment. Finally, a process for obtaining sensor modeling requirements by considering relevant sensor effects is described.

3.1. A structure and study process for physical sensor modeling

This section presents an overview of the sensor modeling process. The objective of the VIVID project is to achieve standardization in both modeling and validation processes.

3.1.1. Process overview

An overview of the suggested modeling process is shown in Figure 3-1, with the logical flow described in the leftmost column. The methodology begins by considering objects and phenomena relevant to the sensors in the physical world, which are identified through multiple ways. These phenomena act as requirements and, at the same time, as reference data for the models.

Next, the modeling process yields models for the environment, the propagation, and the sensor. In order to develop these data-based models, comprehensive measurements of relevant properties are required. To validate a model, a decomposition is applied to first validate model constituents before the integrated model is validated. Both modeling and validation are based on scenarios. The whole process is followed multiple times in an iterative fashion. This allows gradually increasing the complexity of the phenomena and scenarios which are considered.

3.1.2. The role of decomposition

In order to limit the complexity of the task, decomposition is applied at different points in this work. Firstly, the sensor requirements are decomposed into different sensor phenomena. Each phenomenon is understood as a requirement in the sense that the sensor model must capture the respective phenomenon fully and correctly. Further information on the phenomena is provided in section 3.3. Phenomena are decomposed and included in different specific scenarios. Furthermore,

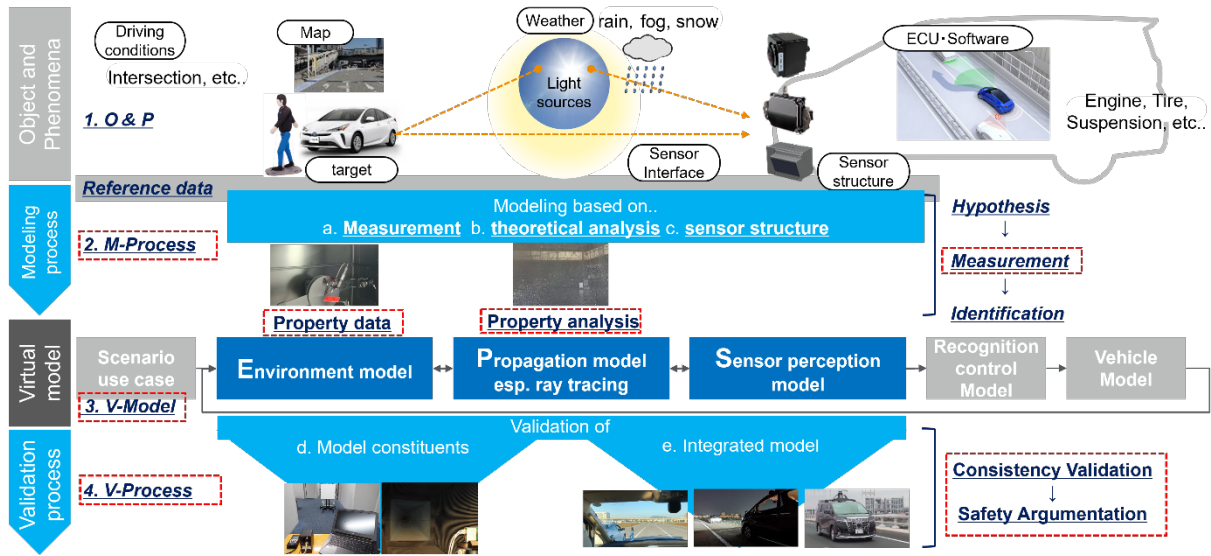


Figure 3-1: Overview of the modeling process; further details provided in the main text

the physical sensor model itself is decomposed into three different aspects. Firstly, an environment model is required to consider the external environment, including both static and dynamic objects. Secondly, the propagation model considers all phenomena related to the propagation of electromagnetic waves between the sensor and its environment. This encompasses for example lighting conditions and weather phenomena which influence the propagation parameters in a sensor-specific way. Finally, the sensor data processing is modeled in the sensor perception model. The environment is further decomposed into different constituents as discussed in section 4.1.

3.1.3. Model development and validation process

Modeling and validation follow an iterative process. Considering different phenomena separately allows to limit and manage the complexity of the task. The phenomena are initially considered under simple conditions, then gradually increased in complexity. The modeling and the validation processes both rely on scenarios which also proceed along increasing complexity. An example for a simple effect related to lidar sensors may be the reflectance of a target. This effect is first studied by simple targets such a Lambertian reflector under laboratory conditions.

Only after obtaining accurate results for the corresponding validation experiments of a single effect without interaction, it is meaningful to move on to more challenging scenarios. This approach ensures that the results remain interpretable since any invalid results obtained by a model in this scenario can be traced back to its origin. The iterative approach ensures that all prior phenomena are validated before moving to more complex scenarios.

The increase of complexity typically follows a high-level structure: Firstly, sensor-specific standardized targets are tested under laboratory conditions. This allows for a precise control of the experimental environment, for example, by utilizing shielded anechoic chambers in the case of radar. Next, static measurements are conducted on proving grounds. Here, the environment can be controlled to a certain degree despite the more realistic environment than in a laboratory setting.

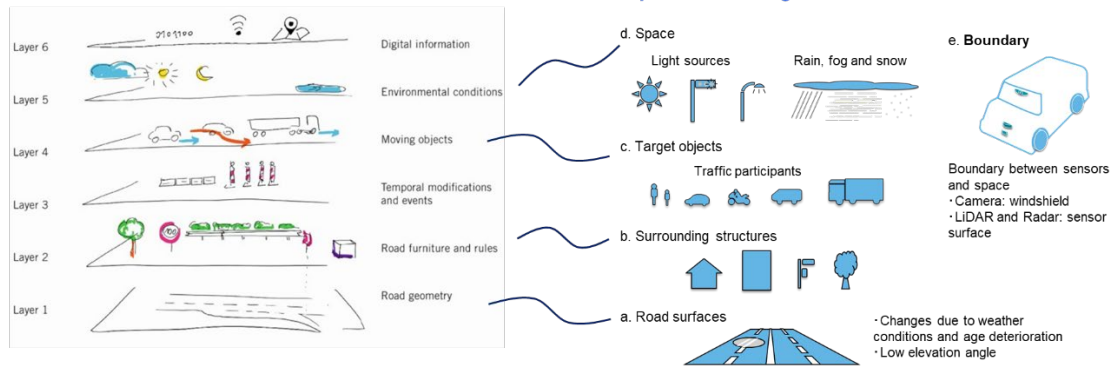


Figure 3-2 Structural decomposition of the environmental model¹⁸ applied in DIVP® and VIVALDI

The static environment may again be explored first using standardized targets. This step is followed by more complex geometric targets such as vehicles. After considering these static scenarios, it is possible to consider dynamic scenarios. Initially, these scenarios remain simple in terms of movement patterns such as driving along a straight line.

Finally, the scope is expanded towards more complex scenarios which emulate realistic traffic situations. Such scenarios are characterized by the presence of multiple time-varying targets, traffic participants, and complex trajectories. Examples include scenarios such as proposed by Euro NCAP¹⁹. Other scenarios intentionally include perceptually challenging factors such as small obstacles (e.g., lost cargo) or dark-clothed pedestrians crossing a road at nighttime.

3.2. Decomposition applied in DIVP® and VIVALDI

In this section, the environmental model is considered as one of the key model constituents, as it is required for any of the sensors discussed in later sections. The environmental model is complex since it encompasses the entirety of factors surrounding the sensor and defining the scenario. Therefore, the VIVID consortium proposes to structure the environmental model into layers. Such an “out-of car” description is a key enabler to realize AD/ADAS sensor-focused validation in the virtual space. Based on the 6-layer environmental model proposed by the German PEGASUS project²⁰ and depicted in Fig. 3-2, VIVALDI & DIVP® defined a sensor-centric space model segmentation consisting of six layers as a common VIVID architecture.

When modeling the assets of each layer, both partner consortia fully leveraged the advantages of their complementary expertise, with VIVALDI providing radar and lidar knowledge and DIVP® focusing on camera knowledge.

¹⁸ Modified from: https://media.springernature.com/lw685/springer-static/image/art%3A10.1007%2F38311-018-0197-2/MediaObjects/38311_2018_197_Fig1_HTML.jpg

¹⁹ European New Car Assessment Programme: Test protocol – AEB Car-to-Car systems, available online: <https://cdn.euroncap.com/media/67887/euro-ncap-aeb-c2c-test-protocol-v40.pdf>

²⁰ M. Scholtes *et al.*, "6-Layer Model for a Structured Description and Categorization of Urban Traffic and Environment," in *IEEE Access*, vol. 9, pp. 59131-59147, 2021, doi: 10.1109/ACCESS.2021.3072739

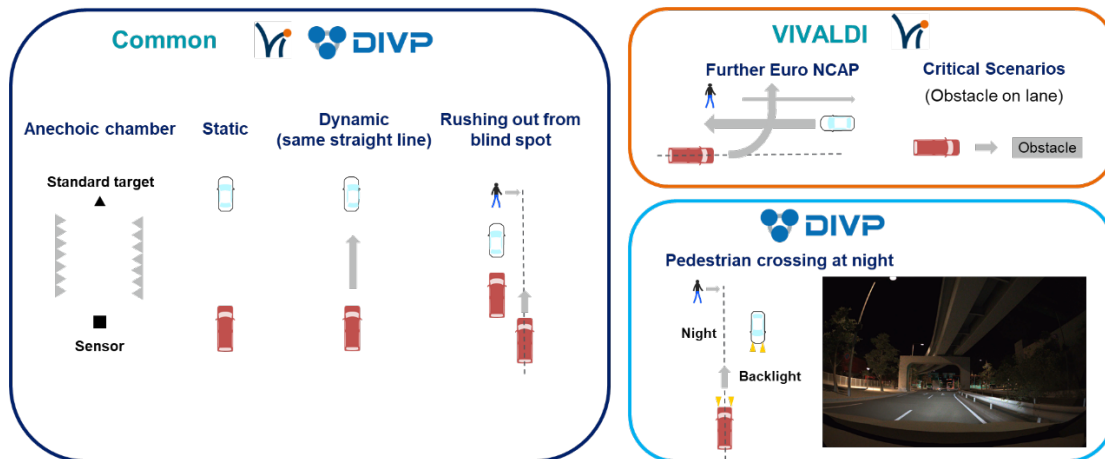


Figure 3-3: Scenarios considered in DIVP® and VIVALDI

Based on the environmental models, VIVALDI & DIVP® undertook joint research about validation scenarios and the modeling approach in each layer. Both consortia agreed on scenarios such as static objects or pedestrians rushing out from a blind spot and mutually exchanged the corresponding parametrizations. Besides common simple scenarios, scenarios based on consideration of risk such as Euro-NCAP scenarios were utilized by VIVALDI and pedestrian crossing in nighttime by DIVP®. Fig. 3-3 illustrates some of these features.

3.3. Extracting requirements from sensor perception effects

Sensor effects are key to the modeling and validation procedure envisioned by the VIVID project. In this section, the process of considering sensor effects to subsequently derive requirements is described.

3.3.1. Sensor perception effects

If real-world scenarios are applied to sensor modeling, the complexity is intractable. The reason is that even a scenario which is typically considered simple in terms of a world model may appear complex for the sensor modeling. An example is a simple highway scenario, where the ego vehicle is travelling alone. However, guardrails on the sides, ground reflections and other multipath effects complicate the modeling of the radar sensor perception. Therefore, the VIVID project proposes to focus on factors which are challenging from a perception viewpoint. These may be different from scenarios which are challenging, for example, for a path planner.

When sensors are utilized, they are subject to various internal and external influencing factors, referred to as cause. An effect is considered a difference in the information contained in the sensor data compared to the condition where a specific influencing factor is absent. A phenomenon is

present if an effect is observable at the sensor output²¹. Accordingly, phenomena are observable deviations with a causal connection to effects. These effects differ for different sensor modalities and even for different designs of one and the same sensor modality. Therefore, it is required to collect and categorize such effects and phenomena as an initial step.

The analysis of the phenomena may take different paths. For instance, experimental evidence documented in literature may be utilized directly. It is also possible to follow an analytical approach and consider relevant equations describing the phenomena. Furthermore, discussions with experts may yield further phenomena for a specific type of sensor. The phenomena should focus on those that are relevant for the intended use case. Accordingly, relevant target phenomena must be defined for the modeling and validation of each sensor modality and implementation individually.

3.3.2. Extracting requirements

The perception phenomena of sensors are directly connected to the sensor model requirements. Let us for example consider ground reflections that a real radar sensor experiences abundantly in road traffic. This effect is required to be included in the respective sensor model. More generally, any relevant environmental effect or phenomenon must be adequately considered by a sensor model, to claim validity. Validity can only be claimed for a specific set of phenomena or for a specified use case.

Accordingly, these phenomena are utilized for the modeling process, but as well for the validation process. For each phenomenon, it is desirable to identify a corresponding scenario which isolates this phenomenon. This allows to model and test specific phenomena separately, which enhances interpretability of the results. The environmental phenomena relating to sensor perception require consideration when designing or selecting a sensor model. Since not all effects can be incorporated into all kinds of sensor models, a suitable choice of model is required. At the same time, these sensor phenomena also require validation themselves. Hereby, the sensor output is first validated for the scenarios which consider specific phenomena in an isolated fashion. Once these are validated, more complex scenarios including multiple causes and phenomena can be considered.

Specific phenomena are associated with causes which are aptly described by physical parameters. For instance, the reflectance of objects can be described by a set of wavelength-dependent geometrical and material parameters. The correct parameter values are determined and verified experimentally, and then leveraged for the modeling of the sensors and the subsequent validation of the sensor model. The validation should be performed independently of the experiments for model parametrization, to ensure reliability of the results.

²¹ C. Linnhoff *et al.*, "Towards Serious Perception Sensor Simulation for Safety Validation of Automated Driving - A Collaborative Method to Specify Sensor Models". 24th International Conference on Intelligent Transportation Systems (ITSC), 2021, doi: 10.26083/tuprints-00018949

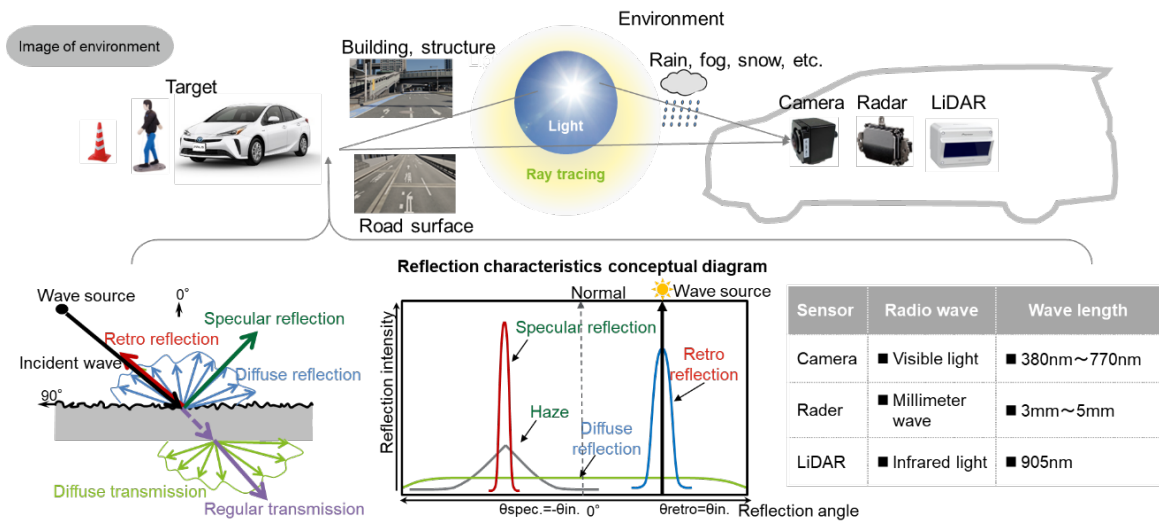


Figure 4-4: Key constituents of environmental and sensor modeling in VIVID.

4. Modeling processes and results

This section details the VIVID modeling processes, namely the modeling of the environment modeling, the propagation, and the sensor. The interfaces enabling an exchange of data and models are considered as well.

4.1. Environment modeling

4.1.1. Introduction

The first constituent of the sensor modeling is the environment modeling, as considered by JT2. For a precise modeling of the environment, physical parameters are required. Material parameters should contain the inherent reflection characteristics for highly consistent sensor perception output. These parameters need to be combined with geometrical parameters (shapes and arrangements), forming a “space design model” that emulates a real environment for precise sensor simulation.

Figure 4-1 depicts the connection between the environment and the sensor, traced back to the physical mechanisms of sensor-specific wave interaction. Besides specular reflections, other types of interaction occur, such as diffuse scattering or refraction, which requires the accurate measurement of material properties in relation to their geometrical appearance such as shape and roughness. In addition, each sensor uses a different range of wavelengths, necessitating decicated measurements. As discussed in section 3.1.2. , the environment is decomposed into layers. For each layer, a static and a dynamic model are created. VIVID worked to provide sophisticated measurement-based assets for these two models.

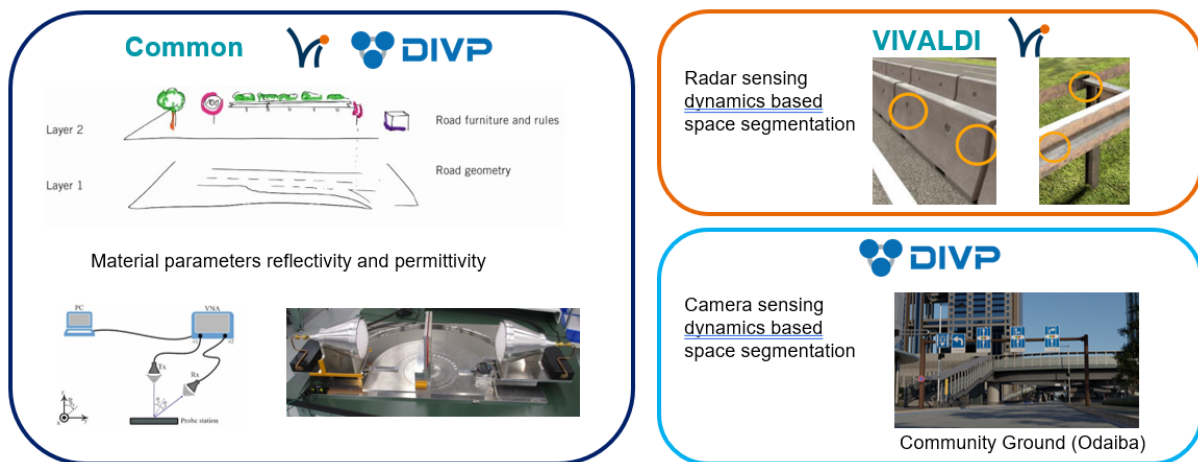


Figure 4-1: Static object model development

4.1.2. Static object modeling

In this section, the material properties of static objects as considered in the layers 1 and 2 of Figure 3-2 are presented. Objects such as road surfaces, road signs, infrastructure, different types of cars and traffic participants are analyzed based on their millimeter wave sensor responses in VIVALDI and camera footage in DIVP®. Both consortia measured the respective physical properties of the segmented material and used them for asset creation. A sketch of the commonalities and complementarities of this approach is provided in Figure 4-2.

4.1.3. Material measurements

In principle, there are two different ways to consider material properties. The first is to determine the dielectric properties and consider roughness separately. The second is to directly measure reflection properties and include them in the wave propagation model. This might be especially suited for materials with a rough surface, since it is possible to measure the specular as well as the diffuse reflection. The former approach is followed by measurements with a waveguide setup, like the one shown in Figure 4-3 on the left side.

The right-hand side of Figure 4-3 shows the schematic of the free-space measurement setup for the reflection properties of a material under test. Reflectivity is measured at different angles-of-incidence, and for the entire frequency band (i.e., for millimeter wave radar from 76 to 81 GHz).

4.1.4. Results

Measurement results were accumulated for different materials including typical plastics, rubber, wood, and asphalt. The values for the rough materials were in good agreement between the German and Japanese partners and consistent with literature data²². Quantitative differences resulted from different sample compositions or roughness. Comparing the data defined in OpenMaterial and the material data recorded in VIVID, we found that some materials

²² V. Kurz, H. Stuelzebach, F. Pfeiffer, C. van Driesten, and E. Biebl. Road surface characteristics for the automotive 77 GHz band. *Advances in Radio Science*, 19:165–172, 2021.

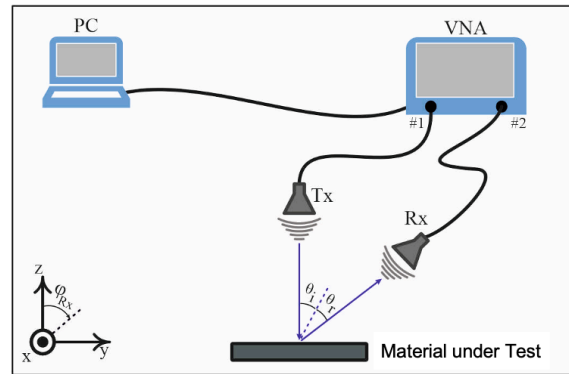
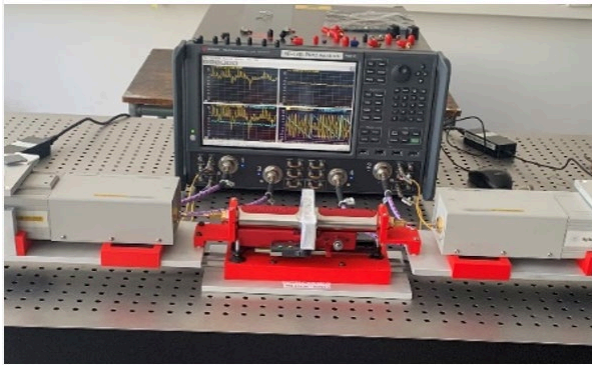


Figure 4-2 : Measurement setup for the determination of the dielectric permittivity (left) and the reflection properties of a material-under-test (MUT) using a free-space setup (right)

used by DIVP[®] and VIVALDI were previously not defined by OpenMaterial and quote the glTF²³ format. Building upon previous work including a glTF format expansion²⁴, all VIVID results have been published on Github²⁵. This is in the interest of the research community as well as the broader automotive industry to ensure that the simulation results obtained by different institutions and companies are comparable. The JT2 has found an agreement to propose the formulation of materials as new items for the ASAM open-standard family. We are convinced that this contributes to sensor validation as a whole.

4.2. Propagation modeling

Besides the interaction of sensor signals with target materials and surfaces, they are affected by the electromagnetic wave propagation in the scenario of interest. These effects can be considered through the propagation modeling²⁶. Figure 4-4 depicts the toolchain of the approach proposed to model precipitation effects such as rain and fog on wave propagation, related to the lidar and radar sensor models. The models were built using the standardized interfaces OSI²⁷ and FMI²⁸ and integrated into the virtual environment CarMaker²⁹. CarMaker provides a ray tracing framework with a bidirectional reflectance distribution function (BRDF) that considers the direction of an incident ray θ , material surface, and wavelength-dependent interaction (e.g., color properties). Both, lidar and radar sensor models used the ray tracing module of CarMaker. The material properties of the simulated objects, the angle-dependent spectral reflectance $R_\lambda(\theta)$, and the reflection types (including diffuse, specular, retroreflective, and transmissive) are specified in the material library of CarMaker.

A functional mock-up (FMU) controller passes the required input configuration to the simulation

²³ <https://www.khronos.org/glTF/>

²⁴ <https://github.com/LudwigFriedmann/OpenMATERIAL>

²⁵ https://github.com/SevdaKIT1234/VIVALDI_Materials/tree/dev/materials

²⁶ Haider, A., Zeh, T., et al. A Methodology to Model the Rain and Fog Effect on the Performance of Automotive LiDAR Sensors. *Sensors* 2023, 23, 6891. <https://doi.org/10.3390/s23156891>

²⁷ <https://www.asam.net/standards/detail/osi/>

²⁸ <https://fmi-standard.org/>

²⁹ <https://ipg-automotive.com/en/products-solutions/software/carmaker/>

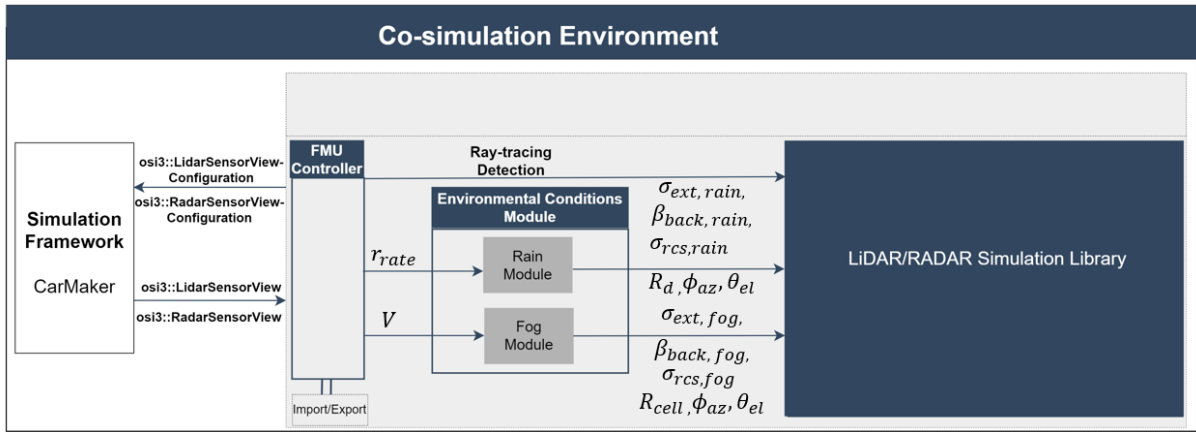


Figure 4-3: Co-simulation framework of the proposed approach to model rain and fog effects in a virtual lidar and radar sensor

framework via the respective `osi3` sensor-view configurations (lidar, respectively radar). The simulation tool verifies the input configuration and provides the ray tracing detections via `osi3` sensor-view reflections. For the lidar sensor, ray tracing data include the time delay τ and relative power P_{rel} . For the radar sensor, the ray tracing data contain the time delay τ , relative power P_{rel} , Doppler frequency f_D , azimuth angle ϕ_{az} and elevation angle ϕ_{el} of each detected ray.

The FMU controller then calls the lidar or radar model and passes the propagation parameters of the detected ray on to further processing. In the next step, the FMU controller calls the environmental condition module and passes the user-selected rain rate r_{rate} or visibility distance V to the rain or fog modules. In the rain/fog module, virtual rain and fog are created, through which the scan module casts the lidar rays according to its scan pattern (ϕ_{az}, ϕ_{el}) , or radar rays are emitted, and a collision detection algorithm is applied to determine whether the transmitted lidar and radar rays hit the rain or fog droplets; if a ray hits a droplet, the backscattered coefficient β_{back} , radar cross-section RCS σ_{rcs} , and the extinction coefficient σ_{ext} based on the drop size distribution (DSD) are calculated. Furthermore, it also provides the spherical coordinates $(R_d, \phi_{az}, \phi_{el})$ of the rain or fog nuclei $(R_{cell}, \phi_{az}, \phi_{el})$ that collided with the lidar and radar rays. Next, the rain/fog module calls the lidar/radar model and passes the rain or fog droplets data on to further processing. The rain module generates virtual rain and computes the extinction coefficient, backscattered coefficient, and RCS. Virtual rain is generated using Monte Carlo simulations. Each raindrop is generated individually based on an underlying DSD and terminal velocity. In this work, we used the Marshall–Palmer rain distributio³⁰ and the large-scale rainfall simulator distribution recorded by a real disdrometer.

4.2.1. Physical rain model

The physical rain model aims at simulating the characteristics of a rain simulator inside the virtual simulation environment. Within VIVID, we conducted systematic measurement campaigns

³⁰ Marshall, J. S., and W. McK. Palmer, 1948: The distribution of raindrops with size. *J. Meteor.*, 5, 165–166.

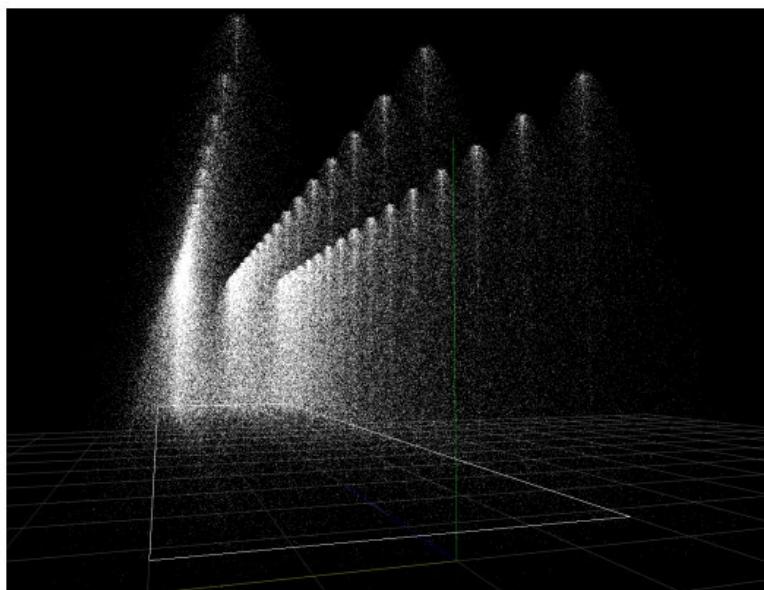


Figure 4-4: Exemplary simulated water drops generated within the white rectangle and shown in white. The column structure results from the drops generated by simulated sprinklers resembling the experimental setup in a real-world rain simulator.

in the two different test facilities National Research Institute for Earth Science and Disaster Resilience (NIED³¹) and CARISSMA³² with a multitude of lidar and radar sensors, including vector network analysis. Based on these studies, we generated virtual rain according to the rain distribution of the NIED rain facility recorded by the real disdrometer. Figure 4-5 shows an exemplary visualization of the rain field generated with the physical rain model.

4.2.2. Interaction between the lidar and radar sensor signals and hydro-meteors

The Mie scattering theory was used to model the interactions between the lidar rays and rain and fog droplets. For radar signal modeling, due to the much larger range of wavelengths, Mie scattering was used to describe the interactions with rain droplets, but Rayleigh scattering was applied to model the effect of fog.

4.3. Sensor modeling

The three sensor modalities camera, lidar, and radar are discussed individually in the following. In each case, the objective is to achieve mutual understanding and interoperability of the DIVP[®] and VIVALDI simulation platform architectures and to discuss required data formats and standardization based on the ASAM open standard interfaces.

4.3.1. Camera sensor modeling (JT3.1)

In order to prove the interoperability between the Japanese and German approaches, data were

³¹ <https://www.bosai.go.jp/e/facilities/rainfall.html>

³² <https://www.thi.de/forschung/carissma/labore/indoor-versuchsanlage-1/>

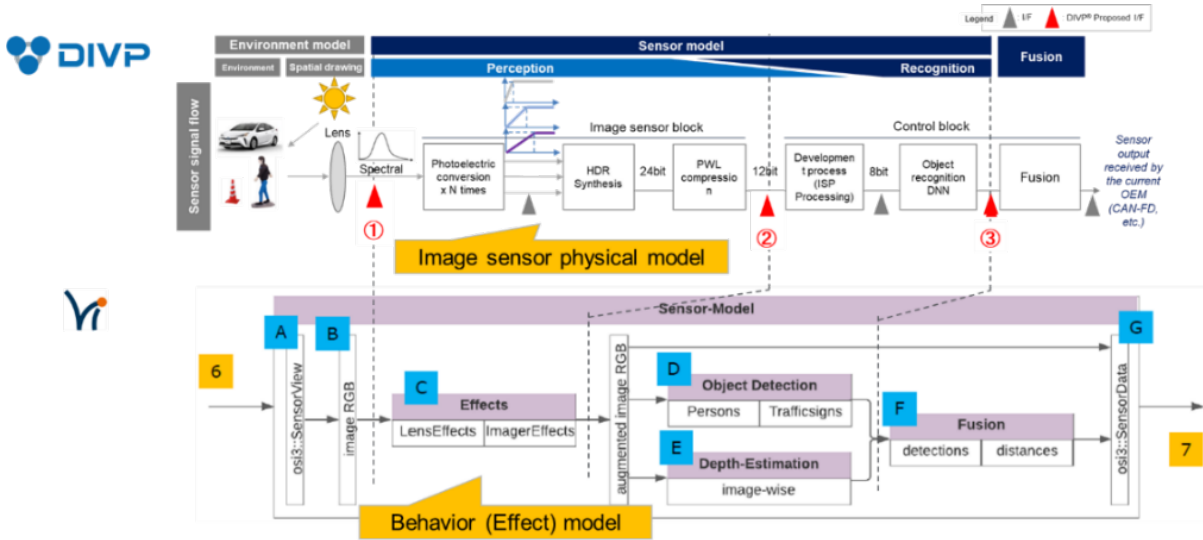


Figure 4-5: Comparison of VIVLADI / DIVP® camera model architectures³³

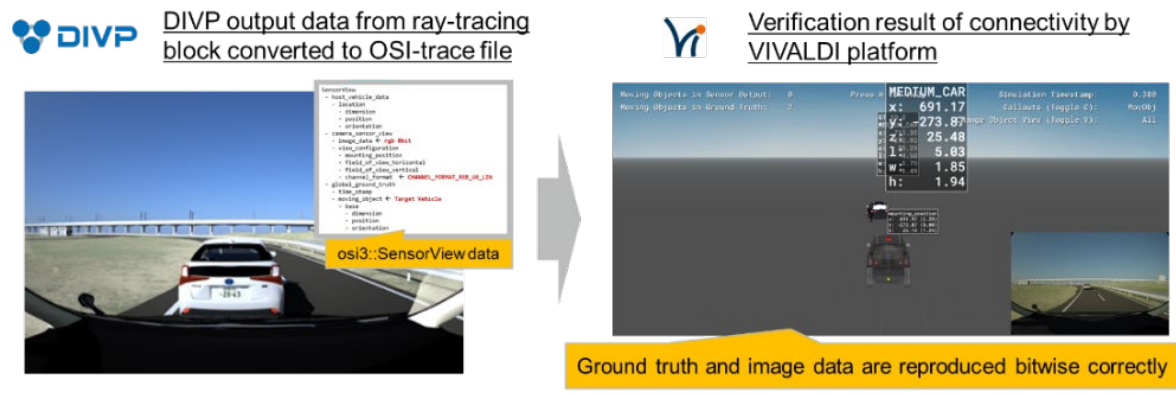


Figure 4-6: Outcome of data exchange activities³⁴

exchanged, followed by verification. Figure 4-6 shows the DIVP® and VIVALDI simulation platform architectures. The main feature of the DIVP® architecture is that it incorporates a physical image sensor model in the perception part, in contrast to the VIVALDI architecture which is based on a behavioral model. Verifying the possibility of data exchange between these different architectures is particularly important to discuss the necessity and utility of interface standardization.

Figure 4-7 illustrates the outcome of the data exchange. DIVP® provided the output data from the camera ray tracing block that were converted from a ROS format to an OSI format (shown on the left-hand side of the figure), then VIVALDI imported the data to their simulation platform. During these activities, the results were fed back, and the data were modified several times, and finally the data import to the VIVALDI platform was verified as shown on the right-hand side of the figure. Through these activities the necessity and the usefulness of interface standardization based on ASAM-OSI was convincingly demonstrated.

³³ Sony Semiconductor Solutions, UAS Kempten
³⁴ Sony Semiconductor Solutions, UAS Kempten



Figure 4-7: Single-frame of simulation environment divp_divp showing traffic sign

In the following, a realistic scenario is considered in which the ego vehicle drives past a traffic sign of diameter 60 cm with a speed of approximately 40 km/h. The corresponding image stream is referred to as real_real. The following four simulations were performed as indicated:

- divp_plain Simulation environment DIVP® without model
- divp_divp Simulation environment DIVP® with DIVP® camera model
- vivid_plain Simulation environment VIVID without model
- vivid_divp Simulation environment VIVID with re-implemented DIVP® model

Furthermore, the camera simulation was verified using a distance estimation algorithm based on image recognition and optical geometry. Results between vivid_divp and divp_divp showed similar patterns, which validates the successful exchange, respectively the equivalent implementation of the model. In addition, an artificial-intelligence model for traffic sign classification was applied. The verification in this case leveraged both classification results as well as the confidence score of the neural network, showing a reasonable agreement of the results.

4.3.2. Lidar sensor modeling (JT3.2)

Figure 4-9 depicts the toolchain and the signal processing steps of the proposed lidar model. The sensor model considers the scan pattern and complete signal processing steps of the sensor type Blickfeld Cube 1³⁵. The model itself was built as an ASAM OSI sensor model packaging (OSMP)³⁶ functional mock-up interface and used the virtual environment of CarMaker. It provides the ray tracing framework with a bidirectional reflectance distribution function³⁷. The lidar FMU model uses the ray tracing module of CarMaker. The material properties of the simulated objects, angle-dependent spectral reflectance $R_\lambda(\theta)$, and reflection types are specified in the material library of CarMaker.

³⁵ <https://www.blickfeld.com/lidar-sensor-products/cube-1/>

³⁶ <https://github.com/OpenSimulationInterface/osi-sensor-model-packaging>

³⁷ IPG CarMaker. Reference Manual Version 9.0.1; IPG Automotive GmbH: Karlsruhe, Germany, 2021.

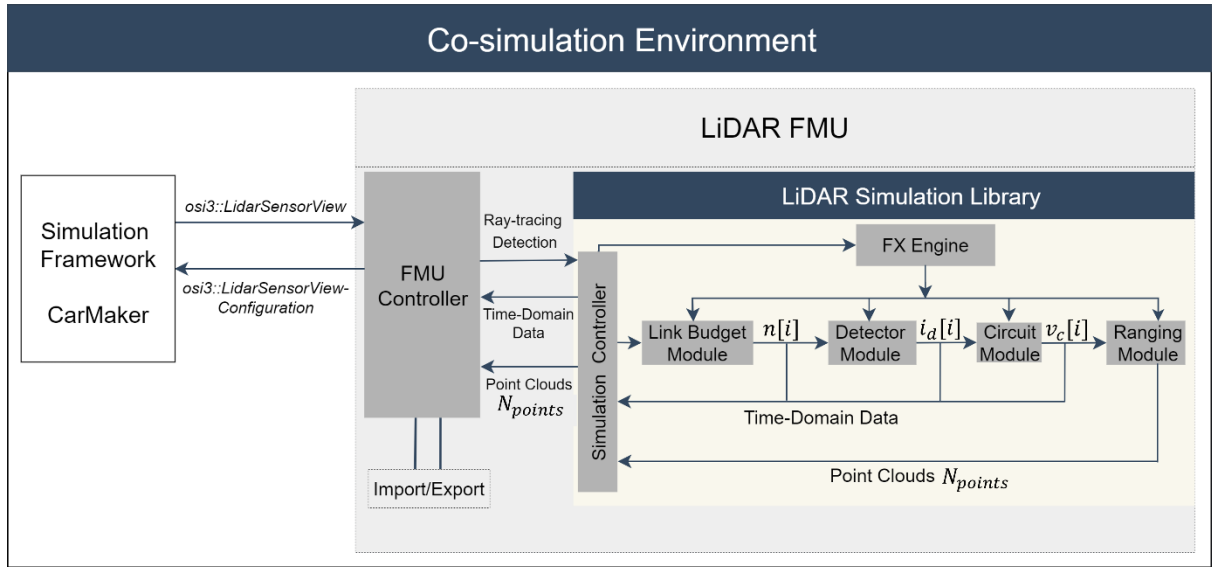


Figure 4-8: Co-simulation framework of the VIVID lidar FMU model

The FMU controller passes the required input configuration to the simulation framework as described above³⁸. Subsequently, the controller calls the lidar simulation library and passes the ray tracing data on to further processing. The central component of the simulation library is the simulation controller. It is used as the primary interface component to provide interactions with the library, for instance, configuring the simulation pipeline, inserting ray tracing data, executing the simulation's steps, and retrieving the results. The next block in the pipeline is the link-budget module, which computes the photons over time.

The task of the detector module is to capture the photon arrivals and convert them into an electrical current signal $i_d[i]$. In the proposed lidar model, we implemented silicon photomultipliers as a detector³⁹. Still, it can also support avalanche photodiode and single-photon avalanche diode detector models. The third block in the pipeline is the circuit module. It amplifies and converts the photo current signal at the detector $i_d[i]$ to a voltage signal $v_c[i]$ that is processed by the ranging module.

The last part of the toolchain is the ranging module, which determines the range and intensity of the target based on the $v_c[i]$ received from the analog circuit for every reflected scan point.

Finally, the effect engine (FX engine) is a series of interfaces that interacts with environmental or sensor-related effects and the blocks of the simulation pipeline. These interactions can involve, for example, the consideration of thermal noise in electrical components, signal attenuation due to weather phenomena, and backscattering.

³⁸ <https://opensimulationinterface.github.io/opensimulation-interface/index.html>

³⁹ Fink, M.; Schardt, M.; Baier, V.; Wang, K.; Jakobi, M.; Koch, A.W. Full-Waveform Modeling for Time-of-Flight Measurements based on Arrival Time of Photons. arXiv 2022, arXiv:2208.03426.

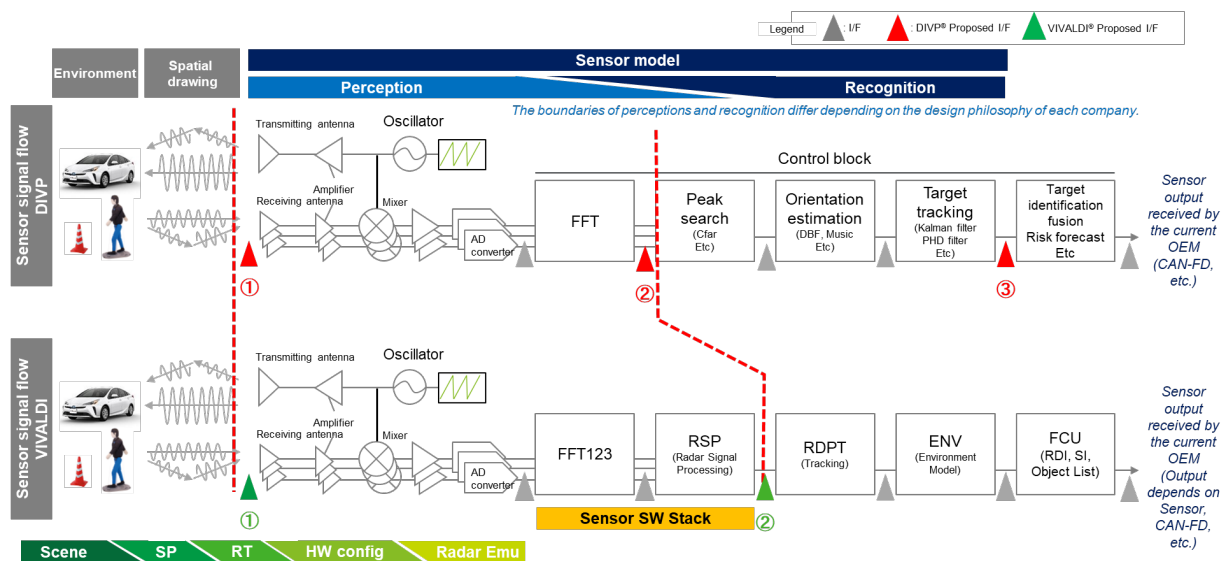


Figure 4-9: Schematic of the VIVID radar sensor model architecture

4.3.3. Radar sensor modeling (JT3.3)

Within VIVID, a multitude of test processes was covered to acquire, emulate, and verify radar sensor models. These include SiL-, HiL-, and even over-the-air ViL-techniques^{40,41,42} enabling the validation of radar sensor models in the installed state. Multiple systematic reference measurement campaigns were conducted at different locations, following a scenario-based approach, in order to provide reliable real-world input data for the modeling process.

A previously existing initial radar sensor model was improved by exploiting the expertise of the project partners and using the opportunity to exchange data with the DVP[®] partners. Mentioned below are some of the salient improvements achieved in the course of the VIVID project.

Figure 4-10 compares the sensor model architectures used by two sister projects. Both sensor models were designed in a way that it is possible to pipe out the output of a particular block in between. This is useful in terms of debugging as well as supporting the data exchange within VIVID. The red triangles represent interfaces along the processing chain where the preferred DVP[®] data format for exchange is located. The green triangles represent the preferred VIVALDI location for data piping and exchange. This setup also enables the protection of intellectual property (IP) by encapsulating the IP-relevant algorithms in each block; the output can be used without having the need to lay bare any confidential algorithms.

To establish successful data exchange, ASAM-OSI was selected as an interface at both points 1

⁴⁰ Sreehari Buddappagari Jayapal Gowdu, P. Aust, A. Schwind, F. Hau, and Matthias A. Hein, „Evaluation of scenario-based automotive radar testing in virtual environment using real driving data“, 2022 IEEE 25th International Conference on Intelligent Transportation Systems (ITSC), doi 10.1109/ITSC55140.2022.9922366

⁴¹ Matthias Hein and Francesco Saccardi, „Automotive Antenna Measurements at VISTA“, Reviews of Electromagnetics, Vol. II, 2023, Roadmap paper, doi 10.53792/RoE/2023/23003

⁴² B. Altinel, E. Asghar, P. Berlt, S. Buddappagari, C. Bornkessel, J. Singh, and M. A. Hein, „Chapter 10 Practical aspects of automotive measurements and virtual-drive testing“, in „Modern automotive antenna measurements“, Lars J. Foged and Manuel Sierra Castaner Eds., Artech House, Boston, London, 2023; ISBN 13: 978-1-63081-849-4

and 2 shown in Figure 4-10 in green. It was discovered that this standard interface, in its present form, was unsuitable for the exchange of radar ray tracing data. Therefore, a new generic ray tracing interface was defined which could be used by both lidar and radar sensor models. The VIVALDI version of this generic interface included the coordinates of the first and the last hit point of the ray, the Jones vector, the path lengths, and the Doppler shifts. These parameters were originally missing. The suggested extension to the OSI interface was submitted as a change request to ASAM, and accepted. The ray tracing interface has meanwhile been integrated into the OSI interface and become available on GitHub⁴³.

Another improvement relates to the sampling strategy of the ray tracer. The sampling method employed by the ray tracer from the industrial partner Continental at the start of the VIVID project was found to need improvement. While the initial sampling method was uniform in 2D space, this was no longer the case after extension into 3D. In order to resolve this issue, the Halton sampling method was chosen in the 2D space. In order to sample a scenario uniformly, the pseudo-random numbers should be progressive, i.e., the number of samples being not fixed and known beforehand, and have low discrepancy, i.e., the distance between samples is maximized.

By not fixing the number of samples a-priori, it was possible to scale-up the resolution dependent on the complexity of the scenario. By additionally maximizing the distance between samples, clumping of multiple sample points within one region and a lower density of sample points in another region could be avoided. Halton sampling satisfied both of the above-mentioned criteria.

Now that the base sampling was assured to be uniform throughout the scenario under study, the next step was to improve the sampling efficiency, in order to minimize the computational time. For example, the scenario might contain regions less relevant for the sensor perception; hence, a lower resolution could be tolerated in that region. Then, other regions may contain targets where a higher resolution is required. The space sampling was initially carried out using the Halton sampling method, after which an AI-trained network decided, based on experience and previous simulations, which the important regions in the scenario were. One obvious factor is that only objects return rays, whereas a ray sent towards the sky would not be reflected. Therefore, the number of rays sent towards the sky could be minimized. Even among different objects, prioritizing vulnerable road users like pedestrians may be prioritized over static objects such as trees.

4.4. Model/data exchange and interfaces for standardization

To prepare safe ADAS/AD systems for later market introduction, the shift to virtual testing – along all types from SiL to ViL – must be intensified. Not all test cases can be verified on proving grounds or in real traffic. Along with this shift, the resources needed for the simulation also need to be considered, in order to complete the development in a reasonable time frame. Therefore, developers need to select the tools and model fidelity according to the specific validation task.

Modular toolchains enhance the exchangeability of simulation tools and models across the various virtual validation environments. This requires common interfaces. In the scope of the two

⁴³ https://github.com/OpenSimulationInterface/open-simulation-interface/tree/689-add_raytracerview_config

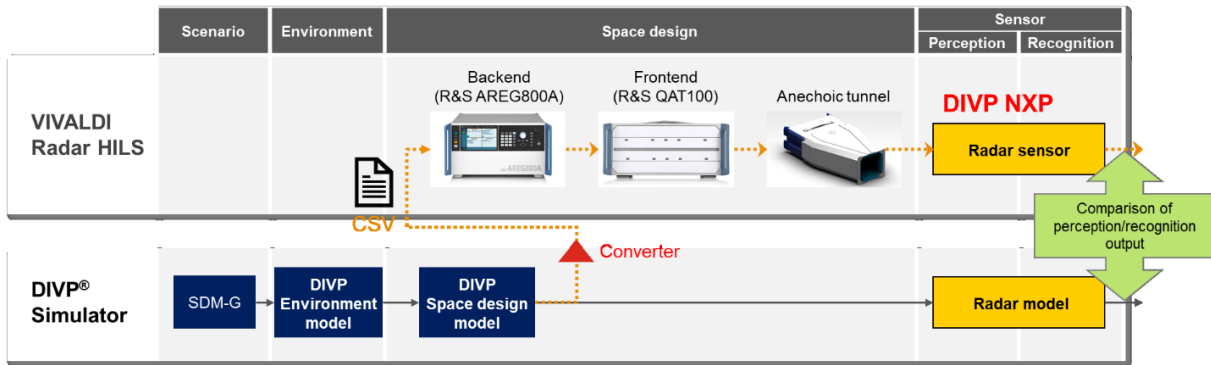


Figure 4-10: Data exchange between DIVP® simulator and VIVALDI toolchain for radar HiL

sister projects, the data/model exchange and discussion of interfaces was achieved for camera, lidar and radar sensors. The exchange of simulation data for radar sensors is described as an example in the following sections.

4.4.1. Exchange of radar sensor simulation data

The DIVP® simulator covers the complete simulation stack from scenario and environment over the space design up to the sensor models. With this, scenarios are simulated and the output of high-fidelity sensor models can be used as input to ADAS/AD functions before deployment to real vehicles.

In the VIVALDI project, instead, HiL and ViL configurations were used as an intermediate validation step between the complete virtual verification and vehicle tests on proving grounds. For the over-the-air (OTA) stimulation of radar sensors, two commercial devices and one research installation (OTA/ViL at VISTA, TU Ilmenau^{40,41,42}) were investigated. As an input, these devices receive the target information from an external environment and sensor simulation (e.g., IPG CarMaker, dSPACE ASM, Vires VTD). As depicted in Figure 4-11, the data were exchanged at this point of the two toolchains employing the commercial test devices. The target information was created by running a defined scenario with the DIVP® simulator and storing the output of the space design model. After converting the data, the recorded scenario could be replayed with the VIVALDI toolchain to the radar HiL setup and stimulate a physical radar sensor.

In parallel, the output of the DIVP® space design model was passed through the radar model and the output of the perception and recognition module was stored. The radar model was designed to match the DIVP® sensor from NXP, which was provided to VIVALDI to be used with the commercial radar stimulators.

The defined csv-file format contains the relative distance, relative velocity and radar cross section for each target within the field-of-view of the sensor. Apart from the target properties, the simulation time step size, coordinate systems of the targets and units need to be aligned to enable a correct replay of the exchanged data.

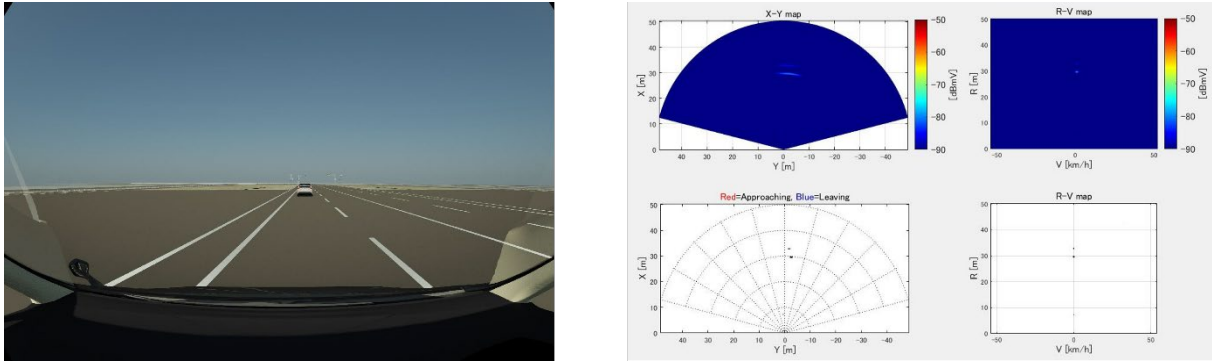


Figure 4-12 Results of the DIVP® simulator for the static radar test scenario

4.4.2. Simulation and measurement results

To compare the output and prove the feasibility of the approach, three static and two dynamic scenarios were chosen. Figure 4-12 illustrates the static scenario of a passenger vehicle placed 30 m in front of the ego-vehicle and the simulated output of the DIVP® radar model.

The results from the DIVP® simulator reveal a clean signal for the passenger vehicle with a low noise level. In comparison, measurements with the real sensor in front of the OTA stimulator showed a significantly higher noise level. Two causes were identified that explain the additional noise – unwanted reflections from the antenna frontend and artificial noise. For stimulation, the radar sensor needs to be placed in front of an antenna array. Although the surface was covered with absorbers and the air gap was shielded by an anechoic housing, the radar sensor would still register detections at the frontend (e.g., from the antenna itself). As these detections are static, in the absence of target stimulation, the radar signal monitoring algorithm would only detect static targets at a distance corresponding to the air gap (e.g. 50 cm). This is typically interpreted as a sensor defect or blindness through contamination and leads to an error state. To prevent this, artificial noise is added by the stimulator.

The results revealed further that the sensor could identify the stimulated target at a distance 30 m, even though noise level and signal amplitude did not match the simulation results. This result demonstrates that the intended use of OTA radar stimulators, namely the testing of ADAS/AD systems with the integrated hardware (sensor, control unit, vehicle) in safety-critical scenarios, can be successfully achieved. Furthermore, the measurements and simulations showed the feasibility of combining the DIVP® simulator with the VIVALDI toolchain and resulted in a common interface description for OTA radar stimulation.

5. Validation process

Having discussed the modeling approach in detail above, we now turn to the validation of these models. As previously discussed, the modeling process consists of the distinct aspects of environment, propagation, and sensor modeling. The validation step is performed with real-world measurements conducted separately from any experiments used to parametrize the models. How-

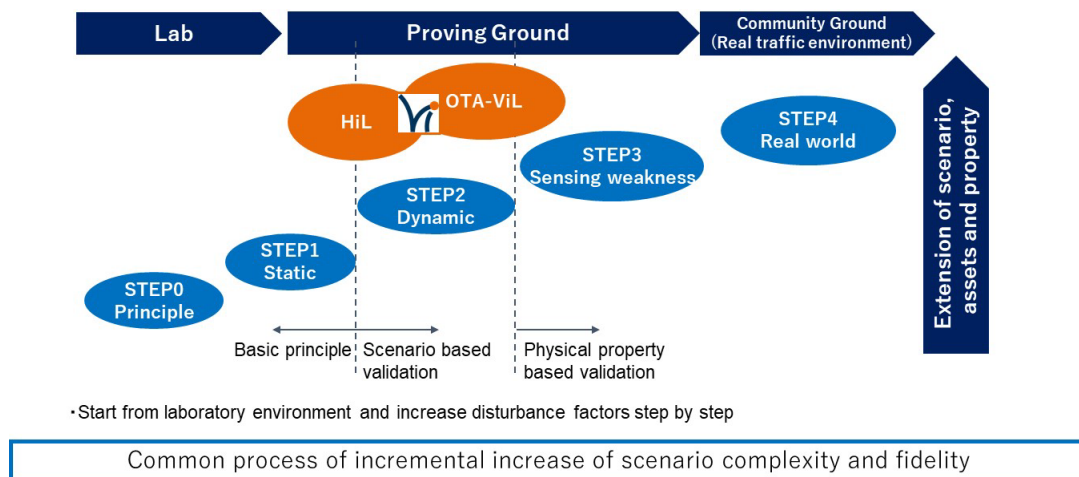


Figure 5-1: Validation process overview

ever, different aspects of sensor modeling are intertwined in a complex manner when considering a typical urban scene. Therefore, VIVID proposes a structured sequential process, in order to manage the complexity. As shown in Figure 5-1, the validation of the individual models is conducted in three phases of increasing complexity. Firstly, static experimental setups in a laboratory environment are validated. This step ensures that the general sensor principles and simple object models are valid. This is followed by experiments on a proving ground, providing more realistic environments than a laboratory, while maintaining simplicity. Furthermore, the environment is controllable. Here, additional effects such as dynamic objects and sensing weaknesses can be easily validated. The final validation step is carried out in real-world settings in actual traffic. Each validation step is conducted only if the prior steps of validation are successfully completed.

Since each scenario is provided to validate specific principles and sensor effects, failing test cases provides interpretable feedback which can be utilized to update the respective models.

5.1. Validation of model constituents (Laboratory)

In order to characterize each sensor modality on the laboratory level as well as relevant environmental model constituents such as road surface material and traffic objects, both VIVALDI and DIVP[®] devised measurement methods that account for the physical principles of operation. As described in Chapter 3, the importance and scalability of the validation is shown by comparing the commonalities and complementarities of VIVALDI and DIVP[®] according to each layer defined earlier (see Figure 4-2).

5.1.1. Validation of the dynamic object model (Layer 4)

As exemplified for the radar measurements sketched in Figure 5-2, dynamic object models, where reflective properties are defined for each asset, were validated through laboratory-based measurements such as full-round radar cross-section (RCS) measurements of typical subjects and objects occurring in road traffic. 3D assets such as cars or powered two-wheelers were modeled

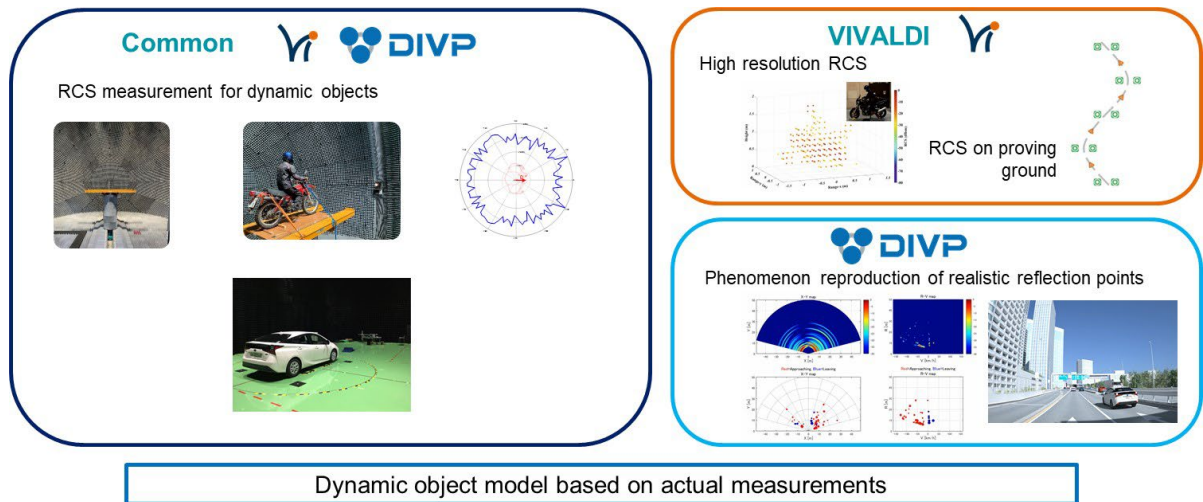


Figure 5-2: Dynamic object model validation (layer 4)

with appropriate body surface geometry and reflectance properties, or sometimes modeled on the basis of dedicated high-resolution monostatic or bi-static RCS measurements. In some cases, surrounding structures were used as stationary objects and in other cases, dynamic objects included to validate the detected radar point clouds between the actual radar-under-test in its installed state and the simulation mode. In any case, static validation of the reflection characteristics of dynamic objects is fundamental and was performed for camera and lidar in the same way.

5.1.2. Validation of environment/space model validation (Layer 5)

In layer 5, weather parameters related to precipitation and lighting conditions, such as rain, fog, snow, sunlight, etc. are defined as scenario components. Since these elements greatly affect the sensor output, the relationship between sensor signal propagation and environmental conditions is important for the model development. Figure 5-3 illustrates the environment/space model development process using rainfall as an example. First, the phenomena such as rainfall and wet road surfaces are analyzed from the viewpoint of each sensor modality based on first principles. Then, the phenomena are measured using equipment that can reproduce the phenomena accurately. Different facilities like NIED⁴⁴ or CARISSMA^{45,46} were used for such studies. NIED's large rainfall experiment station, which has a height of approximately 18 m, was found to reproduce many signatures of natural rainfall. A disdrometer was used to measure characteristic parameters like the particle size, velocity, and integral amount of water density. At the same time, the perceptual and cognitive outputs of each sensor were measured using dedicated sensor setups and test vehicles. The empirical relationships were incorporated into the model by reducing them to analytical expressions to the extent possible.

The model thus created was implemented and checked again for consistency, in order to compose

⁴⁴ <https://www.bosai.go.jp/e/facilities/rainfall.html>

⁴⁵ <https://www.thi.de/forschung/carissma/>

⁴⁶ <https://www.safecad-vivid.net/news/carissma/>

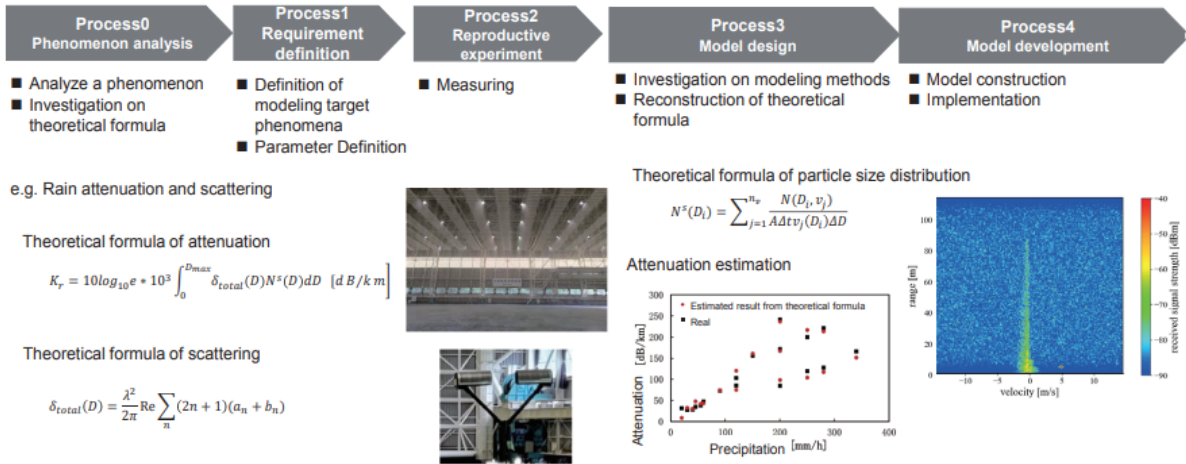


Figure 5-3: Environment/space model development process

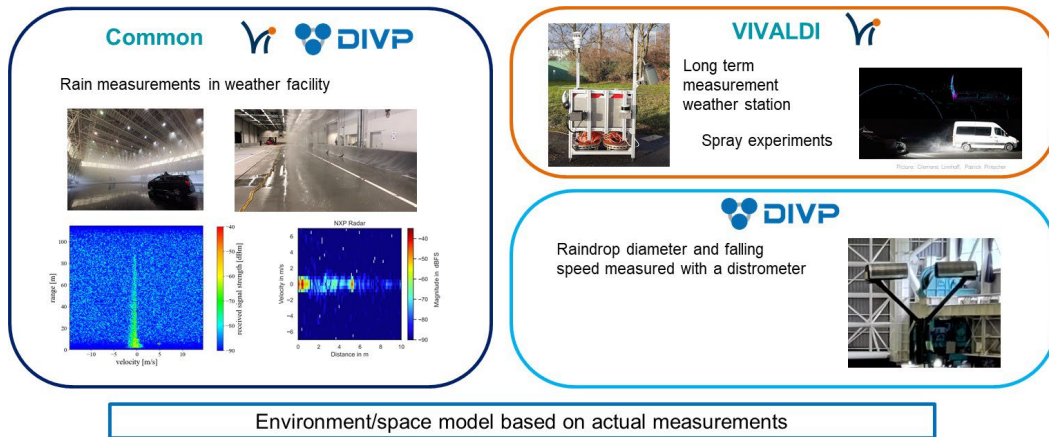


Figure 5-4 : Environment/space model validation (layer 5)

a highly realistic space model. This process remained basically unchanged for both consortia and sensor modalities. In the absence of experimental facilities to reproduce natural phenomena like snow or fog, the sensor signal propagation was first measured by a test vehicle and then put into the modeling process starting from an analytical description of the physical phenomena.

Figure 5-4 reveals the similarities between the VIVALDI and DIVP® approaches for all three sensor modalities. We note that camera, lidar, and radar, even though different brands were applied, could be validated through measurements in the respective facilities. In addition, some partners monitored rainfall in free-space environment with a disdrometer, to examine variations in rainfall conditions. Both consortia studied wheel roll-up caused by rain and snow and are continuing to make progress in their respective fields.

5.2. Validation of the integrated model (installed performance on a real vehicle)

Having validated the individual modeling components, the integrated model needs to be validated as a whole. Within the VIVID cooperation, various test drives with real vehicles were conducted under realistic conditions on proving grounds.

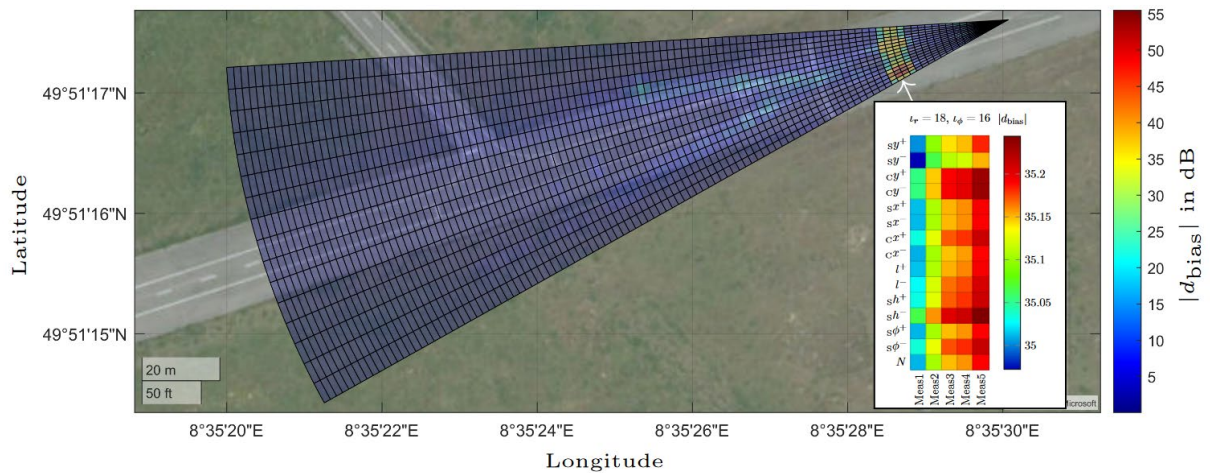


Figure 5-5: Satellite image showing the difference of real and simulated results on radar cube level. The grid shows the distance-azimuth coordinates of the radar sensor, the magnitude of the offsets in radar power is color coded.

For the sake of brevity, this section presents exemplary validation results. These include test drives conducted for radar sensor model validation. Here, the validation was performed at different interfaces of the radar sensor signal processing, including the radar cube, the radar detections and, for specified regions of interest, around objects of interest. An exemplary visualization for the model validation results on the radar cube level is provided by Figure 5-5. Further detailed results and explanations can be found in the corresponding publication.⁴⁷

Other validation experiments were performed for a real vehicle under realistic conditions at the Jtown⁴⁸ proving ground of JARI in Tsukuba, Japan. Exemplary lidar point clouds received from the simulated and real vehicle targets are shown in Figure 5-6. It should be noted that the daylight intensity was recorded and modeled in the simulation environment. We compared the simulated and real test drive results frame by frame, to validate the environment and sensor modeling. Comparisons were performed on multiple interfaces along the perception chain to ensure consistency. This includes a comparison on the point cloud level as well as for the common object detection task as an exemplary recognition task.

On a point cloud level, metrics such as the mean absolute percentage error (MAPE) were applied. For the key performance indicators (KPI) such as the number of points N_{points} and the intensity I_{mean} , an error of 8.83% and 8.90% were obtained, respectively, for all frames of the scenario.

To validate the sensor model at the object recognition level, we trained a state-of-the-art deep learning based PointPillars network⁴⁹ for object detection using simulated lidar data. Then, we tested it with real and simulated data of the vehicle target shown in Figure 5-7. We used the

⁴⁷ Elster, L.; Rosenberger, P.; Holder, M.; Mori, K.; Staab, J.; Peters, S.: Introducing the Double Validation Metric for Radar Sensor Models, 22 June 2023, PREPRINT, <https://doi.org/10.21203/rs.3.rs-3088648/v1>

⁴⁸ <https://www.jari.or.jp/en/test-courses/jtown/>

⁴⁹ Lang, A. H.; Vora, S.; Caesar, H.; Zhou, L.; Yang, J.; Beijbom, O. (2019): PointPillars: Fast Encoders for Object Detection from Point Clouds. In: 2019 IEEE/CVF Conference on Computer Vision and Pattern Recognition Workshops (CVPRW), S. 12697–12705

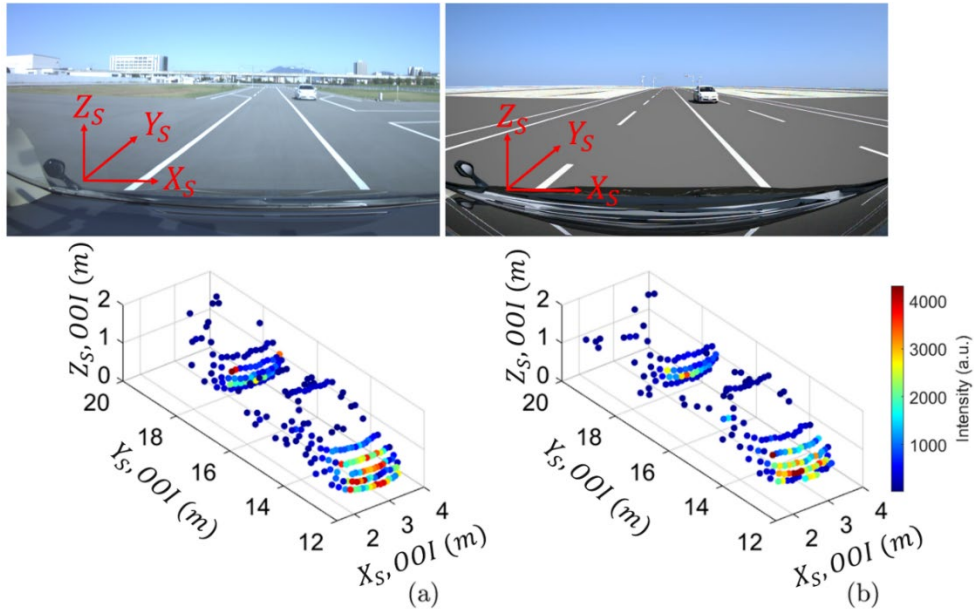


Figure 5-6: a) Exemplary real measured lidar point cloud. b) Exemplary simulated point cloud. The scanning frequency of the real and virtual lidar sensor was 5.4 Hz

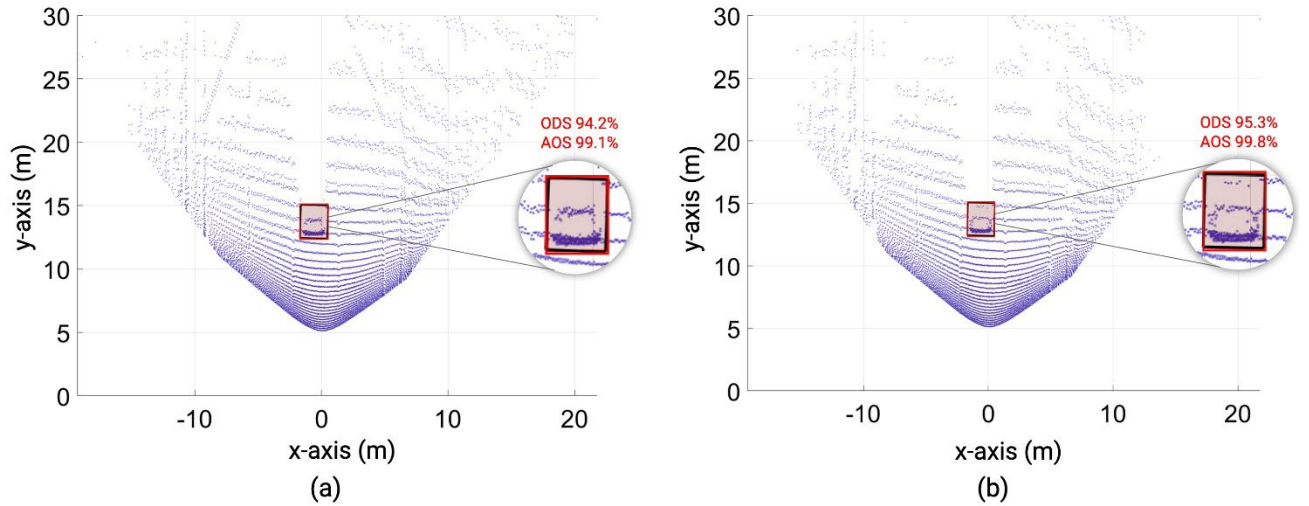


Figure 5-7: a) Real point cloud data: Black and red cuboids represent the ground-truth 3D orientation of the object and the 3D orientation of the object estimated by the object detection algorithm, respectively. (b) Simulated point cloud data: Black and red cuboid

Average orientation similarity (AOS) metric⁵⁰ to find the correlation between the 3D ground truth orientation of the object and its 3D orientation estimated by the object detection algorithm.

Overall, validation results for sensors integrated into the overall vehicles were obtained for all three sensor modalities. The validation procedure for each sensor emphasizes a combination of low-level metrics on sensor data level and high-level metrics considering downstream tasks such as object recognition. The results demonstrated that the procedures refined during testing on simpler

⁵⁰ Geiger, A.; Lenz, P.; Urtasun, R. (2012): Are we ready for Autonomous Driving? The KITTI Vision Benchmark Suite. In: 2012 IEEE Conference on Computer Vision and Pattern Recognition (CVPR), S. 3354–3361.

laboratory scenarios were applicable to more complex validation experiments. Furthermore, it was shown that interpretability can be retained even for complex scenarios including effects from the real world.

5.3. Validation of consistency and safety argumentation

In chapter 3, examples of physical models were described that are highly consistent with real phenomena, including experiments to model each sensor modality. In this section, we summarize the process of validating the consistency of each sensor model. In addition, an explanation of the proposed reflection on the safety argumentation for connected and automated driving is provided.

5.3.1. Consistency validation for the camera sensor model

An overview of the consistency validation for the camera is sketched in Figure 5-8. The camera yields an image, so that the agreement between the model output and the real image can be validated by comparing the output luminance of each RGB for each part of the image. In step 1, a light source is set up and the spectrum and luminance are validated. In an environment with few surrounding structures, such as a proving ground, background light and road surface reflection are added to the process. Here, the RGB luminance output is evaluated. In the evaluation so far, agreement was obtained on a relative level of approximately 20%. In the measurement of RGB luminance under actual vehicle conditions, it is difficult to stabilize luminance due to background light, etc., and there is a 20% variation in luminance arising just from the measurement alone. From this point of view, better agreement is not realistic to achieve. Finally, we evaluated the agreement in the presence of sensor phenomena, such as signal obstruction by the background sunlight on a public road. In this case, we use not only the perception evaluation but also the semantic segmentation recognition evaluation to evaluate the validity of the virtually generated image by validating that the traffic signal cannot be recognized in both real and virtual images. In addition, since there is a need to evaluate the distance measurement algorithm for camera recognition, the relative positions of objects and other objects in the simulated and real images are also included in the consistency validation.

5.3.2. Consistency validation for the lidar sensor model

Similar to radar, the validation process for the lidar sensor model is summarized in Figure 5-9. The target is a point-cloud-type lidar based on time-of-flight, and the consistency between the model output and actual measurements such as distance, angle, intensity, number of points, etc. could be validated successfully.

However, it is necessary to understand the origins of sensor weakness, such as the effect of background light and the response to objects floating in space, such as water or snow bouncing off the wheels, et cetera.

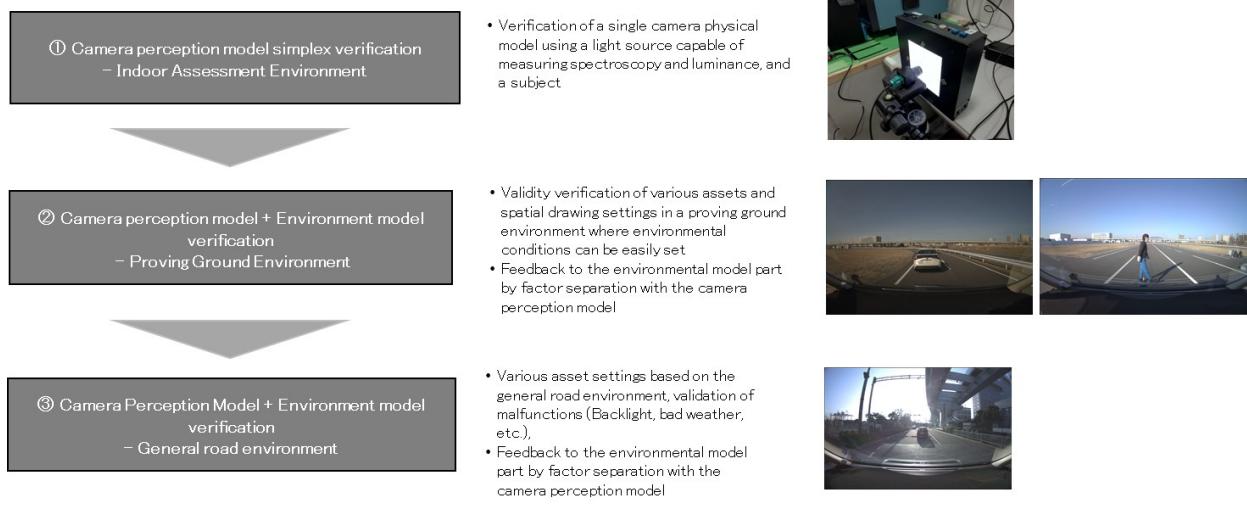


Figure 5-8: Consistency validation for the camera model

Step	Purpose of the verification	Output to be evaluated	validation parameter	validation index
LIDAR Model Consistency verification	<ul style="list-style-type: none"> ■ Evaluate consistency of LiDAR perceptual models (scanning and ranging models) by eliminating errors due to environmental models, spatial propagation models, and scenarios as much as possible 	<ul style="list-style-type: none"> ■ RX Model Output * PSSI LIDAR Only ■ Perceptual model output 	<ul style="list-style-type: none"> ■ Intensity distribution of the received signal ■ Intensity distribution of the noise ■ Angle ■ Distance ■ Intensity ■ Range limit 	<ul style="list-style-type: none"> ■ Consistency of intensity distribution, average and variance at each distance of a target whose shape and reflection characteristics are known ■ Consistency of intensity distribution, average, and variance of noise at each distance of a target whose shape and reflection characteristics are known ■ Vertical resolution (elevation angle between adjacent lines) ■ Consistency of horizontal resolution (azimuth angle between horizontal neighbors) ■ Consistency of accuracy and precision at each distance of a target whose shape and reflection characteristics are known ■ Consistency of detection probabilities of targets whose shape and reflection characteristics are known
Environment Model + LIDAR Model Consistency verification	<ul style="list-style-type: none"> ■ Evaluate the consistency of environmental models and LiDAR perception models (scanning and ranging models) by eliminating errors caused by spatial propagation models and scenarios as much as possible. 	<ul style="list-style-type: none"> ■ Perceptual model output 	<ul style="list-style-type: none"> ■ Distance to target ■ Number of points hit by a target ■ Target Size ■ Intensity of the target point cloud 	<ul style="list-style-type: none"> ■ Consistency of accuracy and precision of distance ■ Consistency of the number of points ■ Consistency of target size ■ Consistency of intensity distribution
Impact assessment on recognition model output	<ul style="list-style-type: none"> ■ Evaluate the effect of the difference between the perceptual model output point cloud and the actual LiDAR output point cloud on the recognition model output. 	<ul style="list-style-type: none"> ■ Recognition model output 	<ul style="list-style-type: none"> ■ Distance detection limit 	<ul style="list-style-type: none"> ■ Detection probability of the target
malfunction reproduction verification	<ul style="list-style-type: none"> ■ Evaluate rainfall / snowfall effects, failure reproduction, consistency verification 	<ul style="list-style-type: none"> ■ Perceptual model output ■ Spatial attenuation model 	<ul style="list-style-type: none"> ■ Number of points hit by a target ■ Intensity of the target point cloud 	<ul style="list-style-type: none"> ■ Consistency of the number of points ■ Consistency of intensity distribution
Extendability verification	<ul style="list-style-type: none"> ■ Reproduction of malfunctions on highly reflective road surfaces and validation of consistency 	<ul style="list-style-type: none"> ■ Perceptual model output 	<ul style="list-style-type: none"> ■ Number of points of white line point cloud ■ Intensity ratio of white line point cloud 	<ul style="list-style-type: none"> ■ Consistency of the number of points ■ Consistency of intensity ratio

Figure 5-9: Consistency validation process and index for the lidar model

Step	Purpose of the verification	Confirmation characteristic	Validation index
Join Behavior Check	<ul style="list-style-type: none"> ■ Validation of Defined I/Fs and Verification of Perceived Output for Point Wave Sources (Corner Reflectors) 	<ul style="list-style-type: none"> ■ Distance, speed, bearing and signal strength ■ antenna directivity and circuit noise ■ Emblem Error 	<ul style="list-style-type: none"> ■ Distance, speed, direction and signal strength in anechoic chamber ■ Direction dependence of signal intensity and signal intensity distribution of noise ■ azimuth measurement error
Pre-verification (Stationary Objects)	<ul style="list-style-type: none"> ■ Verification of basic single targets (Prius, NCAP dummy persons, bicycles) 	<ul style="list-style-type: none"> ■ Reflection intensity and reflection point distribution ■ Multipath due to road surface 	<ul style="list-style-type: none"> ■ Orientation Dependence of Reflection Intensity and Reflection Point Distribution ■ Distance dependence of corner reflector signal intensity
Basic verification (Movable Objects)		<ul style="list-style-type: none"> ■ Micro doppler ■ azimuthal separation capability 	<ul style="list-style-type: none"> ■ Signal Strength Distribution in the Speed Direction by Pedestrian Swing and Tire Rotation ■ Increase in the number of antennas and azimuth separation capability by MIMO
Failure reproduction Verification	<ul style="list-style-type: none"> ■ Verification of spatial attenuation due to rainfall and clutter generation due to raindrop scattering ■ Examination of snow effect, snow road surface clutter 	<ul style="list-style-type: none"> ■ rain attenuation ■ rain scattering ■ Snow attenuation, road clutter 	<ul style="list-style-type: none"> ■ Spatial attenuation relative to precipitation ■ Raindrop shape distribution and clutter distribution ■ Spatial attenuation, clutter intensity and distribution for snowfall
Scalability verification	<ul style="list-style-type: none"> ■ Verification in actual traffic environment ■ Verification of targets (manholes and corrugated cardboard) that are prone to false detection and non-detection by millimeter-wave radar 	<ul style="list-style-type: none"> ■ Reflection intensity and reflection point distribution of peripheral structure ■ Multipath with Tunnel Walls 	<ul style="list-style-type: none"> ■ Signal intensity distribution for distance, speed and direction of tunnels and overpasses ■ Occurrence of ghosts on overtaking vehicles

Figure 5-10: Consistency validation process and index for the radar model

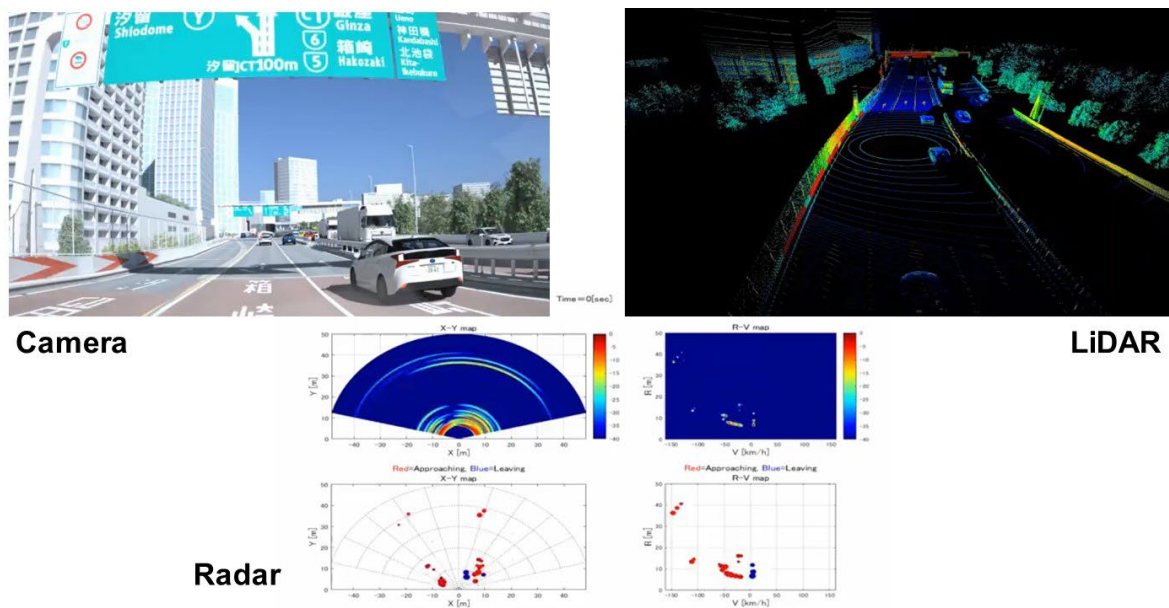


Figure 5-11: Sensor perception by the virtual physical simulator

5.3.3. Consistency validation for the radar sensor model

The radar sensor model was validated with physical values for distance, relative velocity, azimuth, elevation, reflection strength (RCS, radar reflectivity), and antenna noise, as indicated by Figure 5-10. The figure also summarizes the specific sensor weakness phenomena and includes most of the elements of validation agreement: Scattering and attenuation due to rain, point cloud distribution and reflection intensity, road clutter, and so on. The evaluation of sensor outputs for each event using actual vehicles was conducted simultaneously for camera, radar, and lidar, but each sensor requires its own output validation. The radar model was constructed with a high degree of consistency with respect to the real-world reference data.

5.3.4. Safety argumentation through highly consistent physical sensor simulation

Although safety argumentation remains under discussion and has not yet been consistently established, the results of VIVID are likely to contribute to this highly important step.

By implementing the consistency validation process, it is possible to obtain realistic sensor perception outputs from camera, radar, and lidar in a dynamic traffic scenario environment, as shown in Figure 5-11. In other words, it is possible to virtually evaluate the reliability of recognition performance based on fidelity metrics such as shielding rate and intersection-over-union (IoU)⁵¹ to see whether a connected and automated vehicle can obtain the information necessary for safe driving. As described in chapter 2, this can show the validity of the operational design domain (ODD) and control responses in concrete terms based on the evaluation of recognition limits and the resulting performance evaluation of the automatic system in driving scenarios based on various use cases. The dynamic evaluation of the recognition timing can also be used to compute the

⁵¹ Wu, Xiongwei; Sahoo, Doyen; Hoi, Steven C.H. (2020): Recent advances in deep learning for object detection. In: Neurocomputing 396, S. 39–64. DOI: 10.1016/j.neucom.2020.01.085.

subsequent risk of conflict with other traffic participants, and the behavior of the automated vehicle during these driving processes can be explained, making it easy to envision the potential for safety arguments.

6. Summary of key results and conclusions

6.1. Summary of key results

VIVID addressed the key question: *"How can the safety of CAD driving functions be tested, measured, and assured?"* Answers to this question are based on the realistic and accurate modeling of the sensors under consideration, their traffic environment, as well as the impact of the space in between on electromagnetic wave and signal propagation. The methodological structure of the bi-national project aimed at covering essential parts of the multi-dimensional parameter space for scenario-based safety assurance and safety argumentation as illustrated, e.g., by the X-model. The modeling processes were laid out along dedicated scenarios, reaching from simple to complex situations challenging the respective sensor modalities and accounting for the international trend towards virtual testing standards for homologation. The three sensor modalities camera, lidar, and radar were intensely studied, based on comprehensive reference measurements in real-world or proving ground tests as well as through systematic laboratory measurement campaigns. Based on the physical processes, sensor models were successfully composed for each modality, paving the way for future refinements and adaptations to forthcoming improvements of sensor performance. In order to quantify the validity and fidelity of the sensor models, suitable validation metrics have been proposed and applied, following a layered modular and iterative process. This progress lays the ground for comprehensive, fully digital testing based on software-in-the-loop methods. Further refinement of all modeling steps involved and their continuous validation through reference data acquired under real-world conditions will provide a framework that can eventually be used to create reliable virtual reference data to achieve the final goal: Safety assurance of CAD.

The independent yet cooperative efforts of the Japanese and German project consortia have created multiple mutual benefit through their commonalities and complementarities: Concepts to formulate data formats and model interfaces have enabled seamless interoperability between the different simulation toolchains while keeping intellectual property rights safe, accelerated international harmonization, and led to significant standardization efforts following a strict policy of open data, open interfaces, and open standards. Different research priorities and different brands of sensors in different environments have widened the physical modeling ground and thus provided additional fidelity that individual national research efforts could never have leveraged.

6.2. Conclusions

The history of automobile safety began with the world's first accident involving the world's first car, invented by Nicolas Joseph Cugnot in 1769⁵². Although there was an operating device

⁵² "Nicolas-Joseph Cugnot | Facts, Invention, & Steam Car | Britannica". www.britannica.com. Retrieved 9 September 2022.

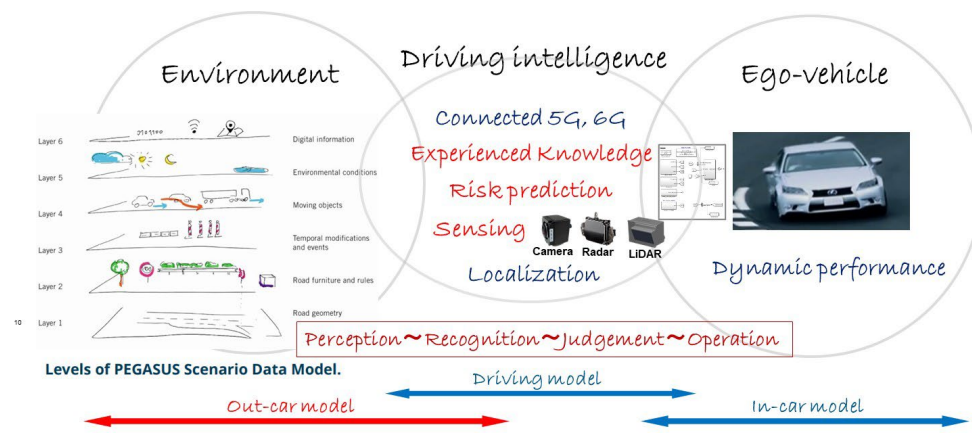


Figure 6-1 From in-car modeling to out-car modeling

equivalent to steering and braking, it did not have sufficient performance to avoid a collision with a wall. Today, the evolution of driving performance, collision safety technology, preventive safety technology, and advanced safety technology using electronic control has overcome the test of time. And now, the "driving intelligence" that has been cultivated through a long history of automobiles, drivers, and traffic environments is about to be replaced by machines and software in the trend towards higher or even full automation, and it is necessary for researchers and developers to understand the significance of these driving histories. In addition, the safety of connected and automated vehicles plays a dual role for the safety of the system itself, which has become more complicated, and the contribution to zero traffic accidents brought about by the system functions.

The VIVID project focused on external sensing, perception, and recognition, which are the keys to highly automated driving systems, and took on the challenge of modeling the environment, propagating space, and sensors. VIVID, together with the PEGASUS project family for driving scenarios, is a very valuable contribution to the safety assurance of self-driving cars in virtual space. According to Figure 6-1, modeling the driving environment including natural phenomena like weather and lighting conditions, and sensor functions of an out-car, which could not be achieved in the conventional model-based design that challenged the integrated modeling of the in-car, was a challenge that required a zero start in terms of creation methods and processes, but was born from discussions among German and Japanese experts on commonalities and complementarities.

While significant progress has been achieved through the VIVID cooperation, many challenging tasks remain still ahead of us and await suitable funding opportunities, in order to let society fully benefit from connected and automated driving at its finest. Among these remaining challenges are:

- Cross-domain test procedures, thoroughly accounting for the complementarities between the different test modalities like SiL, HiL, OTA/ViL approaches and real-world testing
- Generalized modeling approaches, enabling digital twins independent of manufacturer and type, and adaptable to future sensor and data platforms
- High-definition data collection and continuous updating for such digital twins including all relevant electrodynamic interaction properties on sensor-specific appropriate scales

- Data-driven composition of high-fidelity digital twins combining sensors and systems/functions and operational design domains that enable the training of AI networks based on virtual sensor data
- Inclusion of wireless communication and cooperation among sensors, cars, and road infrastructure, based on 5G or 6G standards, enabling additional safety measures of enormous relevance, e.g., by merging sensing modalities with communications,

The reliable quantification of sensor fidelity, systematic strategies for sensor fusion accounting for the complementary limitations and weaknesses of each individual modality, as well as formal methods to derive reliable safety measures on a generic level will eventually form the basis for controlling the risks of highly autonomous transportation systems.

At the end, as coordinators of the two project consortia, we would like to express our respect for the efforts of the researchers on both sides, who have taken time out of their busy schedules to summarize the main points of VIVID activities in this white paper. Although this document is still on its initial maturity level, we have no doubt that it will contribute to the safety evaluation of connected and automated driving vehicles and will be further upgraded based on the results of its application in the future. We would like to greatly acknowledge the manifold valuable contributions to both projects from all partners in Germany and Japan, the wonderful and truly constructive cooperation between all of them, and the wise and generous funding policy of the German Federal Government as well as the Japanese Cabinet Office that enabled this important piece of research.

Hideo Inoue, for the DIVP® consortium, and Matthias Hein, for the VIVALDI consortium